

NATIONAL TECHNICAL UNIVERSITY OF ATHENS
SHIP DESIGN LABORATORY

MASTER THESIS

Simulation of the discharging/loading
procedure of tankers

Author:

Dionysia Chroni

Supervisor:

Prof. Apostolos Papanikolaou

*A thesis submitted in fulfilment of the requirements
for the degree of Master of Sciences*

in the

“MARINE TECHNOLOGY AND SCIENCE”
School of Naval Architecture and Marine Engineering

December 2013

Acknowledgements

I would like to express my deepest gratitude to my supervisor, Professor Apostolos Papanikolaou, for his continuous support, guidance, supervision and patience, which helped me to do my first steps in the field of research study. I could not have imagined having a better advisor and mentor for my MSc thesis.

Interdependence is certainly more valuable than independence. Mr. Timoleon Plessas, PhD candidate at NTUA, was always there when I really needed. With his enthusiasm, and his great efforts to explain things clearly and simply, he helped me a lot.

Beside them, I sincerely acknowledge Dr. Papalamprou (NTUA), Akis Topaloglou and Stefanos Glaros, as always willing to help and give their best suggestions regarding Simulink. I am most grateful to Mr. Adamopoulos and MARAN Tankers for the provision of data for the validation of the model, as well as for his guidance.

It's my fortune to gratefully acknowledge the support of some special individuals. Words fail me to express my appreciation to Dimitris Kazagkas. I am much indebted to him for his valuable advice in my work, spending his precious times to read this thesis and gave his valuable suggestions. Beside him, I acknowledge Panagiotis Kontoulis for the finishing touches. I could not neglect, Mario Mastrokallo, for the valuable assistance in excel diagrams. It is also a pleasure to mention that, I thank all of you, Dimitris K., Marios, Dimitris F., Anastasis, Panagiotis, Vaso and Timoleon for the stimulating discussions, for the sleepless nights we were working together and for all the incredible time we have had. Thanks to all of you, I got the first feeling in academic research.

I would like to express my appreciation to the E.U REFRESH project, for its financial support and knowledge providing to me.

I would like to thank my family: my parents Vasilis and Ifigeneia, my sister Maria and her husband Christo, as well as my niece Kallirroi for supporting me spiritually throughout my life and my MSc research study. Last but not least, I would like to express my deepest gratitude to my boyfriend, Andreas for providing me with unflinching support, continuous encouragement, help and love.

Contents

Acknowledgements	i
1 Introduction - Scope of thesis	1
2 Discharging procedure of crude oil tankers	3
3 The physics of the problem - Basic principles - Physical/mathematical model	5
3.1 Pump Operation	5
3.2 Modified Bernoulli Equation	14
3.3 Impact of Reynolds Number	15
3.4 Darcy - Weisbach Formula	16
3.5 The Moody Chart	17
3.6 Flow friction losses	19
4 Ship Operational Constraints	23
4.1 Back Pressure - Net Positive Suction Head (NPSH)	24
4.2 Consideration of ship's stability and trim	28
4.3 Shear Forces and Bending Moments	32
5 The development of the model at Matlab's Simulink environment	37
5.1 Matlab's Simulink enviroment	37
5.2 The cargo and ballast model	45
5.2.1 Modeling the tanks	45
5.2.2 Modeling the pumps	47
5.2.3 Modeling the pipes, valves and fittings	49
5.2.4 Cargo (crude oil) definition in the model	51
5.3 Measurement station	52
5.3.1 Pumping log and Oil Transfer Plan	52
5.3.2 Ship's stability and strength calculations	56
5.3.3 Energy calculation - Fuel oil consumption	57
5.4 Solver configuration	59
6 Validation of the Model	63
6.1 Case study 1	65
6.2 Case study 2	66

6.3 Case study 3	67
6.4 Results and discussion	68
7 Conclusions/Future work	77
A Physical properties of fresh water	78
B Simulation results	80
Bibliography	91

Dedicated to my grandmother...

Chapter 1

Introduction - Scope of thesis

In recent years the shipping industry suffered by the adverse international economic environment, the steep increase of fuel (bunker) prices and the new regulations (Emission Control Areas [1], water ballast treatment [2], etc.), which have dramatically increased the running cost / profit ratio for ship owners and operators.

To address this situation, the marine industry is focused on the implementation of various energy/cost saving practices (e.g. slow steaming, optimal routing). Besides, new propulsion concepts in the context of main and auxiliary engine installation are introduced, so as specific fuel oil consumption and pollutant emissions to be reduced. These concepts include electric propulsion, prime movers with electronical control of combustion process, and installation of exhaust gas aftertreatment devices. In addition, the reduction of ship's resistance is considered as a crucial matter, thus, experimental investigations including optimization studies of new hull designs, propeller forms, as well as coating materials are required. It is noted that pre-existing proven technologies, e.g. propeller shaft generators characterized by high initial capital investment, are now regarded as potential alternatives [3]. Moreover, ship energy and fuel cost benefits can be attained, whether fleet managers and crew follow procedures aiming at efficient ship charging/discharging operations.

In this context, the present study is focused on the modeling of cargo pumping systems of tankers, so as the overall energy consumption to be optimal. Thus, a new model has been developed, consolidating the structure constraints of the cargo handling system, i.e. the hydrostatic characteristics, and the strength and stability characteristics of the vessel, in order energy efficiency to be optimized during a discharging procedure (see figure 1.1).

The present model is applied on the cargo handling system of a modern AFRAMAX tanker. The calculated results have been validated against the actual ones provided by vessel's operator for a number of discharging operations, with good agreement.

The methodology is based on the mathematical modeling of static and dynamic behavior of the fluid, as it flows through the individual components of the hydraulic system (cargo and ballast piping diagram). This approach contributes to the evaluation of system nominal characteristics, and the optimization of operation during actual service conditions (transient / dynamic response).

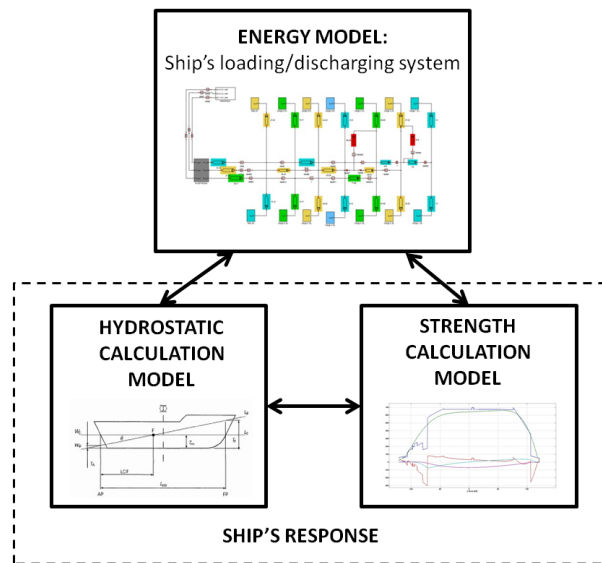


FIGURE 1.1: Flow chart of the model.

Hence, the present model constitutes a decision support tool, which can assist the ship operator to minimize the energy consumption during the cargo discharging:

- by simulating the operation of the existing cargo equipment, in order the overall handling to be optimized during discharging.
- by calculating the payback time in case of an investment including a retrofit modification in the vessel's cargo piping system.
- by evaluating proposals concerning the required number of cargo pumps for newbuild-ing vessels.

A major part of the present thesis was developed within the E.U. funded project RE-FRESH [4]. The support of MARAN Tankers in the provision of data for the validation of the developed model is acknowledged.

Chapter 2

Discharging procedure of crude oil tankers

Discharging oil cargo from a tanker ship requires utmost diligence in planning as well as at safe operation [5].



FIGURE 2.1: Tanker charging/discharging operation.

In this section the basic procedures at various stages of discharging oil cargo from a tanker ship are presented.

In this context, the responsibility for safe cargo handling operations is shared between the ship's Master and the terminal Representative. The manner in which the responsibility is shared should therefore be agreed between them in order to ensure that all aspects of the operations are covered. Thereafter, before starting to discharge cargo, both sides should formally agree (i.e. discharging plan) that the procedure will be followed with safety.

In accordance with the discharging plan, various safety factors should be taken into consideration. Firstly, the inert gas must be set appropriately during the whole procedure in all tanks, in order to maintain a positive gas pressure. As a result, expansion or implosion of the tanks is prevented. Furthermore, the number of cargo pumps which are going to be used and their rotational speed are planned in respect to the maximum and

minimum pressure values at manifolds. A different orientation will lead to a possible failure at both, shore and ship piping networks.

Once all necessary proceedings have been made and the offshore facility is ready to receive cargo, all valves are opened according to the agreed discharging plan. Subsequently, the cargo pumps start to operate at slow speed. The discharge rate is gradually being increased until the pressure at manifolds reaches the values within the agreed limits. After reaching the desired full rate, the pressure at manifolds is being monitored during the discharging operation in order to prevent any fail. In addition, it is worth noting that pumps should operate at their nominal rotational speed in order to ensure system's effectiveness. The reduction of pumps rotational speed leads to a rapid decrease of pumping rate and pumping efficiency. Furthermore, back pressure shall be monitored in order to prevent cavitation that may occur when the pump tries to discharge more cargo than is able to enter the suction. To this end, the systematic control of back pressure as well as the pressure at manifolds is crucial concerning the prevention of any fail at the whole hydraulic network.

However, in actual fact, during the discharging procedure, an instant observation of pressure at manifolds or before pumps may lead to various changes of the discharging plan. For instance, the operation point of pumps, the number of pumps that are used or which valves are opened or closed may change due to shore orders. As indicated above the discharging scenario is a dynamic procedure, which undergoes significant changes during its implementation. As a result, no previous studies are associated with its simulation. It appears that the present development may constitute a substantial step towards reliable engineering.

Chapter 3

The physics of the problem - Basic principles - Physical/mathematical model

3.1 Pump Operation

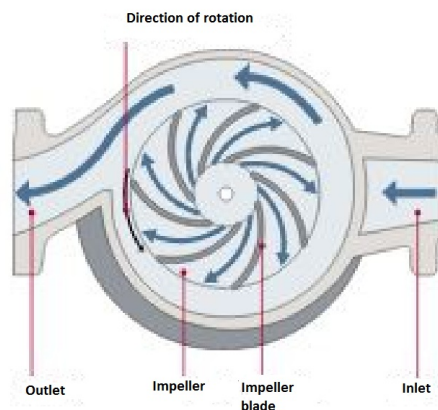


FIGURE 3.1: Fluid path through a centrifugal pump.

Pumps are used to transfer a liquid from one place to another and very often from a low elevation to a high elevation. In addition to the simple movement of the liquid, pumps are also used to increase the flow rate of the liquid. The fluid enters the pump at certain velocity and pressure, which may be even zero. The pump, which consumes a certain amount of energy from an external source, delivers a part of the energy to the fluid in order to increase its energy. Therefore, fluid exits the pump with increased velocity and pressure.

Pumps are of two general types, hydrostatic or positive displacement, and pumps depending on dynamic forces, such as centrifugal pumps. In the present study only centrifugal pumps were considered, which are commonly used in ship's cargo and ballast systems. When a centrifugal pump is in operation, an increase in the fluid pressure from the pump inlet to its outlet is created.

This pressure difference drives the fluid through the system. The centrifugal pump creates an increase in pressure by transferring mechanical energy from the motor to the fluid through the rotating impeller. The fluid flows from the inlet to the impeller center and out along its blades. The centrifugal force hereby increases the fluid velocity and therefore, the kinetic energy is transformed to pressure. Figure 3.1 shows an example of the fluid path through the centrifugal pump [6].

Pump performance is described by a set of curves commonly referred to as the “performance curves” (see figure 3.2). Thereafter, all various information about the head (H), the efficiency (η), the power (P) demand and the NPSH value at different flows, are provided.

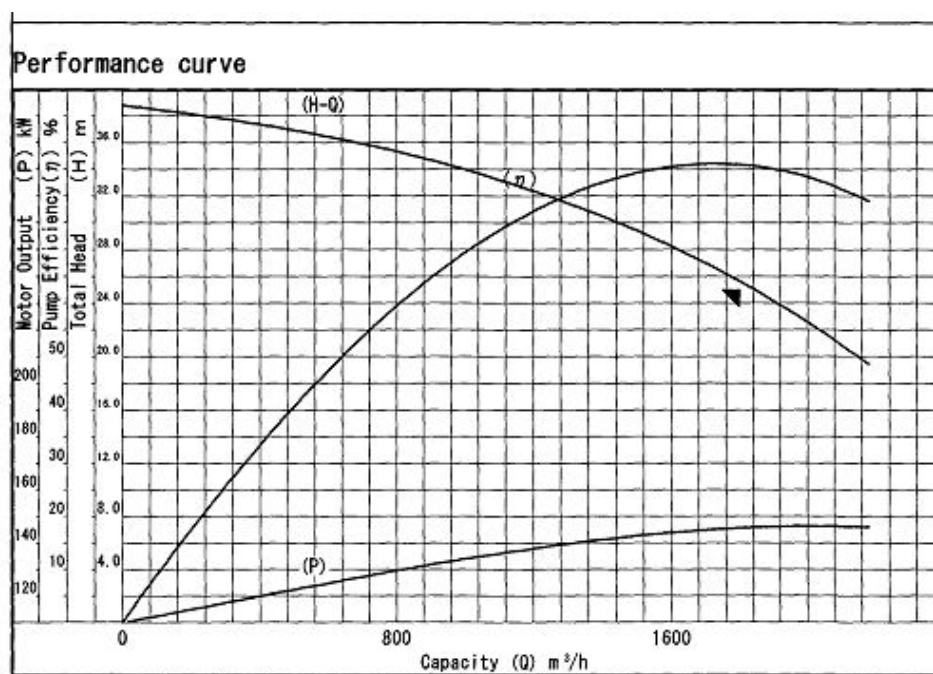


FIGURE 3.2: Centrifugal pump performance curve.

The basic physics of pumping and the individual criteria involved with pumping calculations, as outlined in performance curves, will be analyzed. It is worth noting that, the International Association of Independent Tanker Owners (INTERTANKO) has been published studies [7] about pumping calculations for tanker vessels since for a vessel's performance many disputes have arisen, which tend to be shrouded with the scientific mystic of pumping calculations. In this context, first of all, some common hydraulic terms will be introduced:

Pressure (P) is an expression of force per unit area and is separated into static and dynamic pressure. The sum of the two pressures is the total pressure:

$$P_{total} = P_{static} + P_{dynamic} \quad (3.1)$$

Static pressure is the pressure of a fluid in rest condition. In other words, static pressure is given by the height of a column of fluid above a given point (Head) multiplied by the density of the liquid and the acceleration of gravity (g).

Dynamic pressure is a function of the fluid velocity and can be derived as follows:

$$P_{dynamic} = \frac{1}{2}\rho V^2 \quad (3.2)$$

where

$$\rho = \text{density}\left(\frac{kg}{m^3}\right), V = \text{velocity}\left(\frac{m}{s}\right) \quad (3.3)$$

Pressure is defined in two different ways: absolute pressure or relative pressure.

Relative pressure refers to the pressure of a system related to the barometric pressure. The barometric or atmospheric pressure is the pressure exerted by the earth's atmosphere at any given point and is affected by the weather and the altitude. A positive relative pressure means that the pressure is above the barometric pressure, and a negative relative pressure means that the pressure is below the barometric pressure.

It is worth noting that pressure gauges only measure the relative pressure. As a result, the involved pressures in the pumping calculations of a ship's piping network, are always the relative measured gauge pressures.

Absolute pressure is the pressure that would occur at absolute vacuum [8] and it can only be a positive number.

The conversion from relative pressure to absolute pressure is accomplished by adding the current barometric pressure to the measured pressure ($P_{relative}$):

$$P_{absolute} = P_{relative} + P_{barometric} \quad (3.4)$$

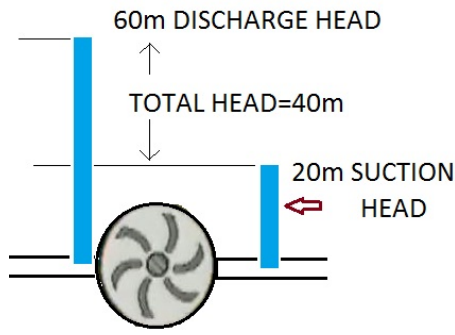


FIGURE 3.3: Total head illustrated as a fluid column.

However, a pump curve (figure 3.2) shows the head (H) instead of pressure, as a function of the flow (Q). Head (H) is the height of the fluid column in the pipe after the pump, as illustrated in figure 3.3. As prescribed, it is common practice to measure the differential pressure across the pump ΔP_{total} , so that the head (H) is calculated as:

$$H = \frac{\Delta P_{total}}{\rho g} \quad (3.5)$$

The **total pressure difference across the pump** is calculated on the basis of three contributions:

$$\Delta P_{total} = \Delta P_{static} + \Delta P_{dynamic} + \Delta P_{geodetic} \quad (3.6)$$

where:

ΔP_{total} is the total pressure difference

ΔP_{static} is the static pressure difference

$\Delta P_{dynamic}$ is the dynamic pressure difference

$\Delta P_{geodetic}$ is the geodetic pressure difference between the pressure sensors

The **static pressure difference** can be measured directly by pressure sensors which are placed at the inlet and outlet of the pump:

$$\Delta P_{static} = P_{stat,out} - P_{stat,in} \quad (3.7)$$

The **dynamic pressure difference** between inlet and outlet of the pump can be calculated as:

$$\Delta P_{dynamic} = \frac{1}{2}\rho V_{out}^2 - \frac{1}{2}\rho V_{in}^2 \quad (3.8)$$

In practice, the flow rate is measured and the pipe diameter of the inlet and outlet of the pump is known, so that:

$$\Delta P_{dynamic} = \frac{1}{2}\rho \left(\frac{Q}{\pi}\right)^2 \left(\frac{1}{d_{out}^4} - \frac{1}{d_{in}^4}\right) \quad (3.9)$$

From equation 3.9 derives that the dynamic pressure difference across the pump is zero if the pipe diameters before and after the pump are identical.

The **geodetic pressure difference** between inlet and outlet of the pump is calculated as follows:

$$\Delta P_{geo} = \Delta z * \rho * g \quad (3.10)$$

where Δz is the difference in vertical position between the outlet and the inlet pipe.

Pumps operation

In this section, an explanation of the pumps operation in a system will be given. Furthermore, the combination of several pumps in the same application will be introduced. Finally, the affinity rules which describe the consequences of certain changes in the pump geometry and speed will be analyzed [9].

A hydraulic system with a single pump

There are systems where fluid is to be transferred from one level to another. These systems are described by two characteristic curves, commonly referred to as the system characteristic curve and the pump characteristic curve (see figure 3.4).

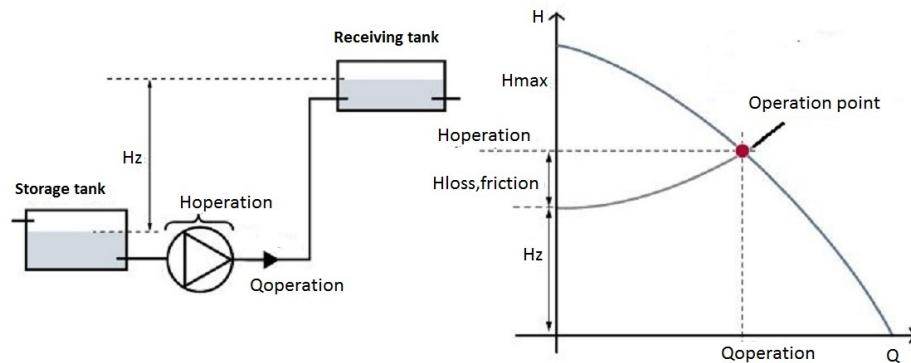


FIGURE 3.4: Example of a hydraulic system with a single pump. The characteristic curves of system and pump are also included.

In this context, regarding the system characteristic curve, there is a constant pressure difference between the two tanks, corresponding to the height difference. This causes an additional head which the pump must overcome. Thus, the characteristic curve of the system goes through $(0, H_z)$. Furthermore, as the flow rate of the system increases, the total head, which corresponds to the friction losses in the pipes, increases proportionally with the square of the flow rate as illustrated in figure 3.4.

As far as the pump curve is concerned, the energy added to the fluid (H) is partly lost due to the friction losses in the pipe system as well as to the mechanical losses in the pump impeller. Thus, as the flow rate of the system increases, the energy given to the system by the pump (H), decreases proportionally with the square of the flow rate.

The operation point of the system is found where the pump curve and the system characteristic curve intersect (see figure 3.4).

A hydraulic system with two pumps operating in parallel or series

In this section, the effects due to the different connections of multiple pumps in a system will be shown. In systems with large variations in flow and a request for constant pressure, two or more pumps can be connected in parallel. The effectiveness of the parallel connection has many operational advantages. The connection of two or more pumps in parallel instead of installing one big pump increases the total efficiency of the system. For instance, the total pump output is usually necessary for a limited period of time due to the prevention of cavitation. Consequently, a single large pump, will typically operate at lower efficiency. In contrast to the operation of a single pump, the operation of smaller pumps which are connected in parallel, can be controlled to operate at the best efficiency point.

In figure 3.5, a system with parallel connected pumps and its corresponding characteristic curve is presented.

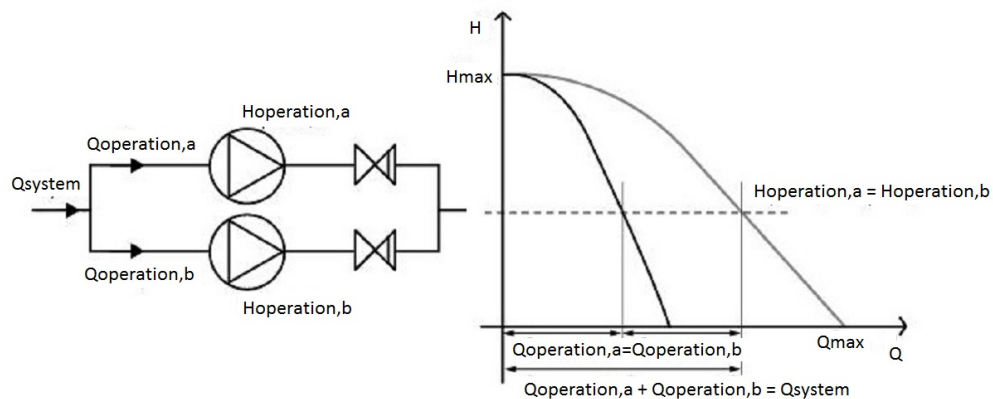


FIGURE 3.5: Example of a hydraulic system with two pumps operating in parallel. The characteristic curves of the pumps are also included.

The pumps connection in series is used in order to overcome a larger head loss than a single pump, for the same flow rate. It is worth noting that the inlet to the second

pump is the outlet of the first pump, so that the head produced by both pumps is the sum of the individual heads, as illustrated in figure 3.6. To this end, the pumps must be identical.

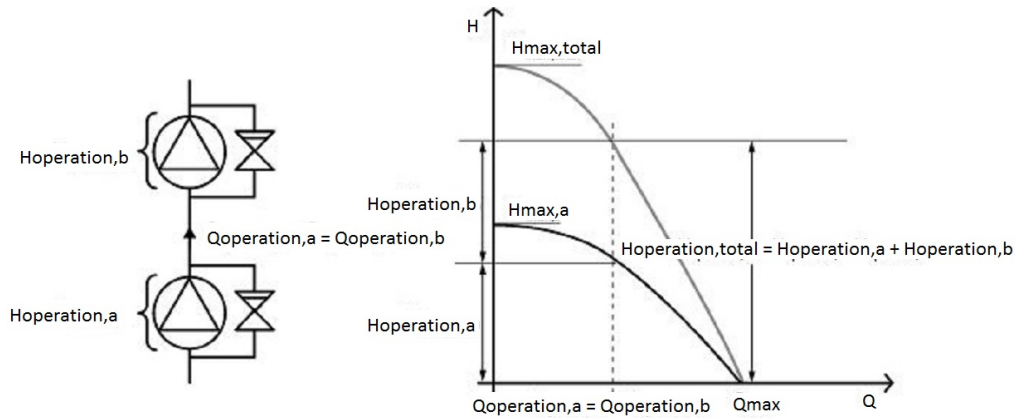


FIGURE 3.6: Example of a hydraulic system with two pumps operating in series. The characteristic curves of the pumps are also included.

The affinity rules

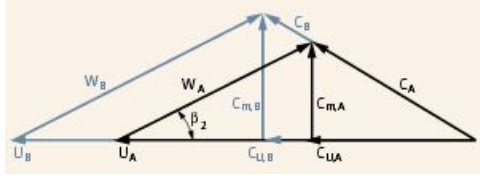


FIGURE 3.7: Velocity triangles.

The affinity rules [10] describe the consequences of certain changes in pump geometry and speed. Affinity rules are derived under the condition that the velocity triangles are geometrically similar before and after a change (see figure 3.7). Thus, the mathematical expression for the relation of the velocities is given by:

$$\frac{U_B}{U_A} = \frac{C_{m,B}}{C_{m,A}} = \frac{C_{u,B}}{C_{u,A}} \quad (3.11)$$

It is worth noting that index A refers to the original geometry and index B to the scaled geometry.

The tangential velocity equals to the rotational speed (n) multiplied by the impeller's diameter D_2 . Therefore, the ratio of similarity between the tangential velocities for different rotational speeds as well as impeller diameters is given below:

$$\frac{U_B}{U_A} = \frac{n_B D_{2,B}}{n_A D_{2,A}} \quad (3.12)$$

As a result, the changes in flow, head and power consumption can be expressed as follows:

Regarding the flow:

$$Q = A_2 C_{2m} = \pi D_2 b_2 C_{2m},$$

$$\frac{Q_B}{Q_A} = \frac{\pi D_{2,B} b_{2,B} C_{2m,B}}{\pi D_{2,A} b_{2,A} C_{2m,A}} = \left(\frac{D_{2,B}}{D_{2,A}}\right)^2 \left(\frac{b_{2,B}}{b_{2,A}}\right) \frac{n_B}{n_A},$$

$$Q_B = Q_A \left(\frac{n_B}{n_A}\right) \quad (3.13)$$

Regarding the head:

$$H = \frac{U_{2,A} C_{2U,A}}{g},$$

$$\frac{H_B}{H_A} = \frac{U_{2,B} C_{2U,B} g}{U_{2,A} C_{2U,A} g} = \left(\frac{D_{2,B}}{D_{2,A}} \right)^2 \left(\frac{n_B}{n_A} \right)^2,$$

$$H_B = H_A \left(\frac{n_B}{n_A} \right)^2 \tag{3.14}$$

Regarding the power consumption:

$$P = Q \rho U_2 C_{2U},$$

$$\frac{P_B}{P_A} = \frac{Q_B \rho U_{2,B} C_{2U,b}}{Q_A \rho U_{2,A} C_{2U,A}} = \left(\frac{D_{2,B}}{D_{2,A}} \right)^4 \frac{b_{2,B}}{b_{2,A}} \left(\frac{n_B}{n_A} \right)^3,$$

$$P_B = P_A \left(\frac{n_B}{n_A} \right)^3 \tag{3.15}$$

3.2 Modified Bernoulli Equation

The modified Bernoulli Equation represents the conservation of energy principle applied to steaming fluids [11]. More specifically, in a steady flow, the sum of all forms of mechanical energy in a fluid along a streamline is the same at all points on that streamline. Therefore, the sum of kinetic energy and potential energy must remain constant. In most flows of liquids and gases at low Mach number (less than 1), the density of a fluid parcel can be considered to be constant. Therefore, the fluid can be considered to be incompressible. For a non-viscous, incompressible fluid in steady flow the Euler equation 3.16, which governs the motion of an incompressible, inviscid fluid, becomes the Bernoulli's equation 3.17, which is valid at any arbitrary point along a streamline [12]:

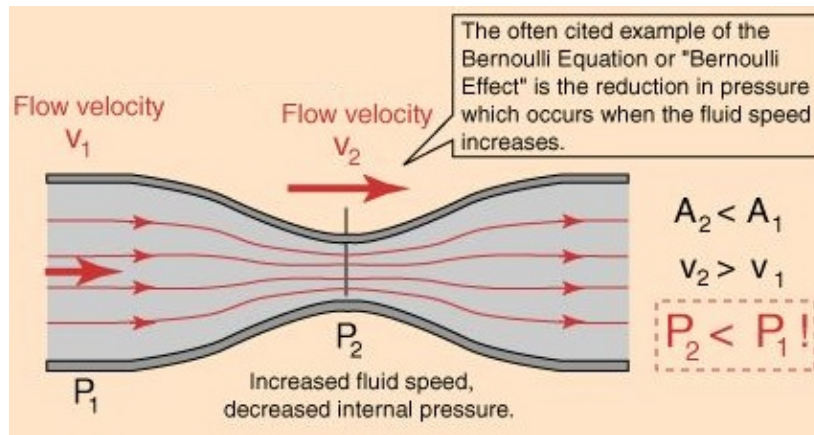


FIGURE 3.8: Flow through pipe.

$$\frac{Du}{Dt} = -\frac{1}{\rho} \nabla P \quad (3.16)$$

where u , P and ρ denote the velocity, the pressure and the density respectively (see figure 3.8).

$$\frac{u_{out}^2 - u_{in}^2}{2} + g(h_{out} - h_{in}) + \frac{P_{out} - P_{in}}{\rho} = constant \quad (3.17)$$

where:

\mathbf{u} is the fluid flow speed at a point on a streamline,

\mathbf{g} is the acceleration due to gravity,

\mathbf{z} is the elevation of the point above a reference plane, with the positive (direction pointing upward) so in the direction opposite is the gravitational acceleration,

p is the pressure at the chosen point, and
 ρ is the density of the fluid

As indicated above, Bernoulli's equation is valid if the following conditions are met:

- **Stationary flow** - no changes over time
- **Incompressible flow** - valid for most liquids
- **Loss-free flow** - ignores friction losses

3.3 Impact of Reynolds Number

Reynolds dimensionless number expresses the ratio of inertial to viscous forces. Reynolds number equals to the velocity multiplied by the characteristic length divided by the kinematic viscosity of the fluid.

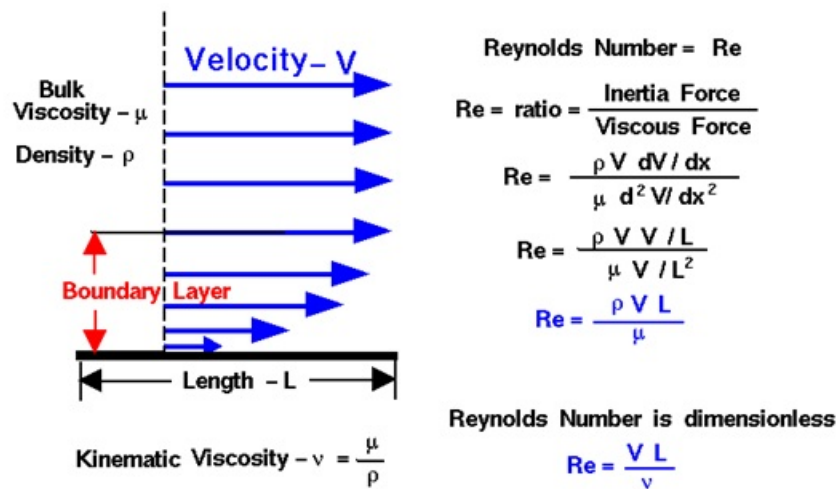


FIGURE 3.9: The velocity profile near wall and Reynolds number definition.

The Reynolds Number is used to determine if the flow is laminar, transient or turbulent. The limits of the specific flow regions are illustrated below:

- **laminar** when $Re < 2300$
- **transient** when $2300 < Re < 4000$
- **turbulent** when $Re > 4000$

3.4 Darcy - Weisbach Formula

When a liquid flows through a pipe, the pressure drops. This pressure drop is caused by the viscous forces within the liquid and by the turbulence that occurs along the internal walls of the pipe, caused by the roughness of the pipe material. This resistance is usually known as pipe friction and is measured on meters head, thus the term head loss is used to express the resistance to flow.

Many factors affect the head loss in pipes, such as the viscosity of the fluid, the size of the pipes, the roughness of their internal surface, the changes in elevations within the system and the total length, which the fluid has traveled within the pipeline. The resistance through various valves and fittings will also contribute to the overall head loss.

In a well designed system the resistance through valves and fittings will be a minor significance to the overall head loss. Over the years excellent progress has been made in developing methods for determining the pressure drop when fluids flow through straight pipes. Industry has converged on the Darcy-Weisbach method (equation 3.18), which is remarkably simple considering the scope of applications that it covers. Darcy-Weisbach equation based on experimental data and is the most accurate and commonly used equation.

$$h_f = f_D \frac{L}{D} \frac{V^2}{2g} \quad (3.18)$$

where:

h_f is the head loss due to friction

L is the length of the pipe

D is the hydraulic diameter of the pipe (for a pipe of circular cross section, this equals the internal diameter of the pipe)

V is the average velocity of the fluid flow, equal to the volumetric flow rate per unit cross-sectional wetted area

g is the local acceleration due to gravity

f_D is a dimensionless coefficient called the Darcy friction factor. It can be found from the Moody diagram or more precisely by solving the Modified Colebrook equation

3.5 The Moody Chart

The Moody chart or Moody diagram (see figure 3.10) is a graph in non-dimensional form that relates the Darcy-Weisbach friction factor, Reynolds number and relative roughness for fully developed flow in a circular pipe. It can be used for estimating pressure drop due to friction with the pipe walls. This is accomplished by using the Darcy-Weisbach formula. If the flow is transient i.e. $2300 < Re < 4000$ the flow varies between laminar and turbulent flow, the friction coefficient is not possible to be determined. The friction factor can be interpolated between the laminar value at $Re = 2300$ and the turbulent value at $Re = 4000$. The Moody Diagram represents the different solutions of the

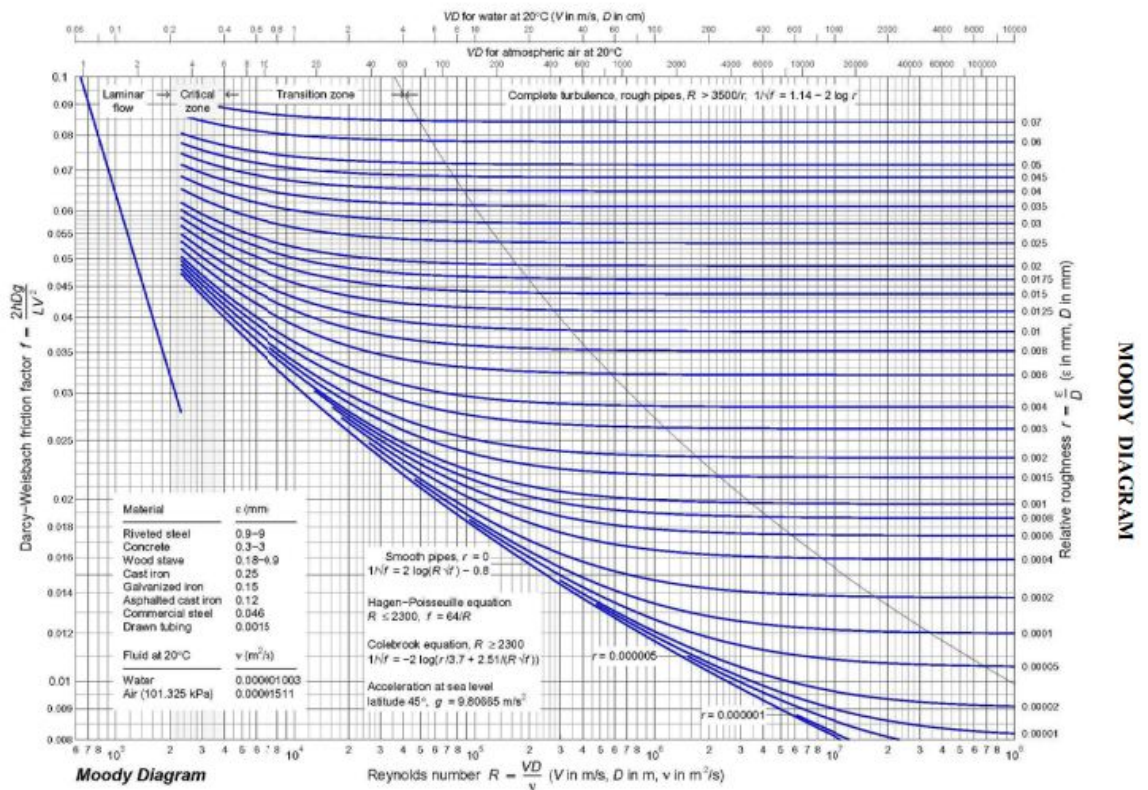


FIGURE 3.10: Friction factors for any type and size of pipe. (From Pipe Friction Manual, 3rd ed., Hydraulic Institute, New York, 1961).

Colebrook Equation (equations: 3.19, 3.20, 3.21). The Colebrook equation is an implicit equation that combines experimental results of studies of turbulent flow in smooth and rough pipes. There are at least three forms of the Colebrook Equation that can be found

in current literature on hydraulics, as shown below:

$$\frac{1}{\sqrt{f}} = -2 \log_{10} \left(\frac{\varepsilon}{3.7D} + \frac{2.51}{R\sqrt{f}} \right) \quad (3.19)$$

$$\frac{1}{\sqrt{f}} = 1.74 - 2 \log_{10} \left(\frac{2\varepsilon}{3.7D} + \frac{18.7}{R\sqrt{f}} \right) \quad (3.20)$$

$$\frac{1}{\sqrt{f}} = 1.14 - 2 \log_{10} \left(\frac{D}{\varepsilon} - 2 \log_{10} \left(1 + \frac{9.3}{R \frac{\varepsilon}{D} \sqrt{f}} \right) \right) \quad (3.21)$$

where:

f is the friction factor

ε is the absolute roughness

D is the inside diameter of the pipe

R is the Reynolds Number

Note that $\frac{\varepsilon}{D}$ is the Relative Roughness.

3.6 Flow friction losses

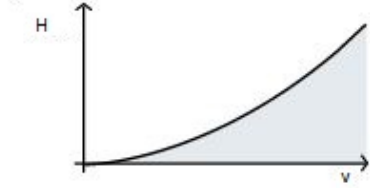


FIGURE 3.11: Friction loss as a function of the flow velocity.

Flow friction occurs in all components of a hydraulic system, such as pipes, valves and fittings. Generally, the flow friction is typically calculated in the same way as the pipe friction loss, expressed as the pressure loss coefficient (ζ) multiplied by the dynamic head into the component (equation 3.22).

$$H_{loss,friction} = \zeta H_{dyn} = \zeta \frac{V^2}{2g} \quad (3.22)$$

The friction loss grows quadratically with the flow velocity, as shown in figure 3.11.

The calculation of flow friction according to the type of each component, corresponds to three different methods: the flow coefficient f for pipes, the equivalent length $\frac{L_e}{D}$ for valves, elbows and fittings and the resistance coefficient K for gradual area change. Furthermore, the pressure loss coefficient (ζ) can be expressed, according to each individual method, as follows:

- **pressure coefficient for pipes:** $\zeta = f \frac{L}{D}$
- **pressure coefficient for valves, elbows and fittings:** $\zeta = f \frac{L_e}{D}$
- **pressure coefficient for gradual area change:** $\zeta = K$

Friction coefficient f for pipes

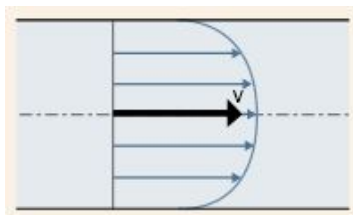


FIGURE 3.12: Parabolic velocity profile inside pipe.

Pipe friction is the energy loss which occurs in a pipe. At the wall, the fluid velocity is zero whereas it attains a maximum value at the pipe center (parabolic profile). The velocity differences which appear along the pipe, see figure 3.12, lead fluid molecules to rub against each other. Therefore, the kinetic energy transforms to heat energy which can be considered as lost.

The friction loss in pipes depends on the fluid velocity, the hydraulic diameter of the pipe, the length and the surface roughness. To this end, the head loss can be calculated as follows:

$$H_{loss,pipe} = f \frac{LV^2}{D2g} \quad (3.23)$$

where f is the friction coefficient, L is the length of the pipe and D is the pipe diameter.

The friction coefficient is not constant but depends on whether the flow is laminar or turbulent (see chapter 3.3). In this context, when the critical Reynolds number is lower than 2300 then flow is laminar and the corresponding friction factor value is independent of the surface roughness. As a result, the friction factor is only a function of the Reynolds number $f = \frac{64}{Re}$. In addition, in case of turbulent flow, the friction factor is estimated by the Moody's Diagram (see chapter 3.5) taking into consideration the Reynolds number and the pipe roughness.

The vessel's piping commonly consists of steel pipes with roughness about 0.1 to 0.2 mm. Furthermore, it is worth noting that the friction increases in old pipes because of corrosion and sediments. Thus, the roughness of pipes in a vessel over the years increases from 0.1 to 0.3 or more mm.

Equivalent length method for bends, elbows and fittings

This method is based on the assumption that the pressure drop, equals to the flow friction losses due to elbows, valves or fittings, can be exposed as a length of a straight pipe, hence the name "equivalent length". Thus, the head loss can be calculated as follows:

$$H_{loss,pipe} = f \frac{L_e V^2}{D2g} \quad (3.24)$$

Moreover, experimental data [13] results that if the equivalent lengths, for a range of sizes of a given type of fitting (for example, a 90° long radius bend), are divided by the diameters of the fitting, then an almost constant ratio is obtained. Therefore, the tabulation of equivalent length data can be easily implemented, since a single data value is sufficient to cover all sizes of that fitting. Some typical data are shown in figure 3.13 for a few frequently used fittings:

TABLE 3.13: Equivalent length of straight pipe for valves and fittings (<http://www.engineeringtoolbox.com>).

Equivalent Length of Straight Pipe for Valves and Fittings (m)												
Screwed Fittings		Pipe Size										
		1/4	3/8	1/2	3/4	1	1 1/4	1 1/2	2	2 1/2	3	4
Elbows	Regular 90 deg	0.7	0.9	1.1	1.3	1.6	2.0	2.3	2.6	2.8	3.4	4.0
	Long radius 90 deg	0.5	0.6	0.7	0.7	0.8	1.0	1.0	1.1	1.1	1.2	1.4
	Regular 45 deg	0.1	0.2	0.2	0.3	0.4	0.5	0.6	0.8	1.0	1.2	1.7
Tees	Line flow	0.2	0.4	0.5	0.7	1.0	1.4	1.7	2.3	2.8	3.7	5.2
	Branch flow	0.7	1.1	1.3	1.6	2.0	2.7	3.0	3.7	4.0	5.2	6.4
Return Bends	Regular 180 deg	0.7	0.9	1.1	1.3	1.6	2.0	2.3	2.6	2.8	3.4	4.0
Valves	Globe	6.4	6.7	6.7	7.3	8.8	11.3	12.8	16.5	18.9	24.1	33.6
	Gate	0.1	0.1	0.2	0.2	0.3	0.3	0.4	0.5	0.5	0.6	0.8
	Angle	3.9	4.6	4.6	4.6	5.2	5.5	5.5	5.5	5.5	5.5	5.5
	Swing Check	2.2	2.2	2.4	2.7	3.4	4.0	4.6	5.8	6.7	8.2	11.6
Strainer		1.4	1.5	2.0	2.3	5.5	6.1	8.2	8.8	10.4	12.8	

Resistance Coefficient K

A gradual area change, such as a gradual cross-sectional area change impacts the flow of fluid. Thus, a resistance represents a gradual enlargement (diffuser) if fluid flows from inlet to outlet, or a gradual contraction (nozzle) if fluid flows from outlet to inlet. The pressure loss coefficient K is determined according to the A.H. Gibson equations:

$$K_{GE} = \begin{cases} k_{cor} \left(1 - \frac{A_S}{A_L}\right)^2 2.6 \sin \frac{a}{2} & \text{for } 0 < a \leq 45^\circ & (3.25a) \\ k_{cor} \left(1 - \frac{A_S}{A_L}\right)^2 & \text{for } 45^\circ < a < 180^\circ & (3.25b) \end{cases}$$

$$K_{GC} = \begin{cases} k_{cor} 0.5 \left(1 - \frac{A_S}{A_L}\right)^{0.75} 1.6 \sin \frac{a}{2} & \text{for } 0 < a \leq 45^\circ & (3.26a) \\ k_{cor} 0.5 \left(1 - \frac{A_S}{A_L}\right)^{0.75} \sqrt{\sin \frac{a}{2}} & \text{for } 45^\circ < a < 180^\circ & (3.26b) \end{cases}$$

where:

K_{GE} is the pressure loss coefficient for the gradual enlargement, which takes place if fluid flows from inlet to outlet.

K_{GC} is the pressure loss coefficient for the gradual contraction, which takes place if fluid flows from outlet to inlet

K_{cor} is a correction factor

A_S is the small area

A_L is the large area

α is the enclosed angle

Furthermore, in case of sudden enlargement or contraction the above equations are transformed to:

$$K_{SE} = K_{corr} \left(1 - \frac{A_S}{A_L}\right)^2 \quad (3.27)$$

$$K_{SC} = K_{corr} 0.5 \left(1 - \frac{A_S}{A_L}\right)^{0.75} \quad (3.28)$$

where:

K_{SE} is the pressure loss coefficient for the sudden enlargement

K_{SC} is the pressure loss coefficient for the sudden contraction

Chapter 4

Ship Operational Constraints

In the present chapter, several constraints which govern the simulated hydraulic procedure of the cargo and ballast discharging operation will be presented.

The prevention of back pressure is crucial for every hydraulic system consisting of a piping network and pumps. The basic principles and the corresponding terms which describe the back pressure will be defined in section 4.1.

The vessel's response, for all loading conditions during the simulation will be considered. It is worth noting that vessel's response is divided into two major groups, namely, the stability and the strength calculations. In this context, the calculations of trim and draught alterations are presented in section 4.2 with respect to the constraints which were determined in the ship's "Trim and Stability Booklet". Moreover, the shear forces and bending moments calculations are presented in section 4.3, taking into consideration the maximum allowable limits in still water condition as assigned by the American Bureau of Shipping [14].

4.1 Back Pressure - Net Positive Suction Head (NPSH)

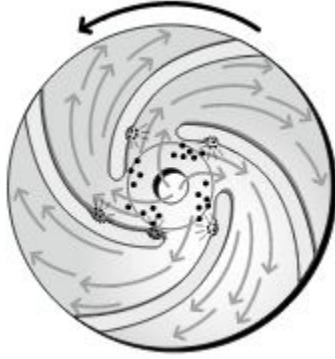


FIGURE 4.1: Cavitation at the "eye" of the impeller.

The drop of pressure of the fluid at the pump's suction to its vapor pressure results to the creation of vapor bubbles. The vapor bubbles will be maintained in the fluid as far as the pressure remains in low level. Therefore, at the time in which the velocity will decrease, the fluid pressure will rise and the created vapor bubbles will move to regions with higher pressure, such as the blade edge at the impeller as shown in figure 4.1. As a result, the vapor bubbles will condensate, so that energy will be released as heat. Thus, the burning and the corrosion which occurs, appears as pitting of the surface which is called cavitation. Furthermore, cavitation causes noise and vibration, which are undesired and harmful.

Net Positive Suction Head (NPSH) is a term which describes the conditions that are related to cavitation.

In this context, distinction needs to be made between the two different NPSH values: $NPSH_A$ and $NPSH_R$.

$NPSH_A$ stands for NPSH available and is an expression of how close the fluid in the suction pipe is to vaporization. Thus, the difference between the total head on the suction side of the pump and the liquid's vapor pressure at the actual temperature defines NPSH available as follows:

$$NPSH_A = \frac{p_{total,in} - p_{vapour}}{\rho g} \quad (4.1)$$

The first term of equation 4.1, $\frac{p_{total,in}}{\rho g}$ is referred to the total head (h_s) at the suction side of the pump.

The suction head in the fluid close to the impeller, based on the energy equation (see Bernoulli's equation 3.17), can be expressed as the sum of the static and the velocity head:

$$h_s = \frac{p_s}{\gamma} + \frac{v_s^2}{2g} \quad (4.2)$$

where:

h_s is the suction head close to the impeller

p_s is the static pressure in the fluid close to the impeller

γ is the specific weight of the fluid equals to its density multiplied with the acceleration of gravity ($\rho * g$)

v_s is the velocity of the fluid

g is the acceleration of gravity

The second term of equation 4.1, $\frac{p_{vapour}}{\rho g}$ is referred to the head which derives from the vapor pressure of the fluid at a specific temperature and can be calculated as follows:

$$h_v = \frac{p_v}{\gamma} \quad (4.3)$$

where p_v is the vapor pressure. It is worth noting that, vapor pressure can be found at “Fluid’s characteristic data tables”. For instance, energy institute provides characteristic data tables for almost all crude oils [15]. Furthermore, in case of water, the vapor pressure value at a specific temperature can be found in the tables of ”Physical properties of water” (see appendix A).

The conjunction of equations 4.2 and 4.3, leads to the following expression of $NPSH_A$:

$$NPSH_A = h_s - h_v \text{ or } NPSH_A = \frac{ps}{\gamma} + \frac{v_s^2}{2g} - \frac{p_v}{\gamma} \quad (4.4)$$

The Required $NPSH_R$ stands for NPSH required and is an expression of the lowest NPSH value which is required for the acceptable operating conditions.

The required $NPSH_R$, for a particular pump, is calculated experimentally and given by the pump manufacturer. It is worth noting that the required $NPSH_R$ increases with the square of the capacity (see figure 4.2) .

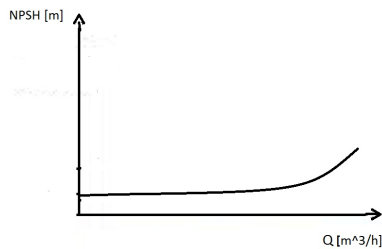


FIGURE 4.2: NPSH characteristic curve of a centrifugal pump.

The available $NPSH_A$ of a system should always exceed the required $NPSH_R$ in order to avoid cavitation of the impeller.

$$NPSH_A > NPSH_R \quad (4.5)$$

The risk of cavitation in systems can be reduced by applying the following precautions:

- For open systems, the pump can be fitted in a lower level compared to the water level
- For closed systems, the system pressure could be increased
- The suction line can be shortened in order to reduce friction losses.
- The suction line's cross-section area can be increased in order to reduce fluid velocity and thereby to reduce friction.
- The temperature of the fluid can be lowered in order to reduce its vapor pressure.

To this end, all necessary calculations, required in order to ensure that no cavitation will occur in a simple hydraulic system are shown in the following example:

Example - Calculation of $NPSH_A$

The system is consisted of an open tank full of water and a pump, as illustrated in figure 4.3. The distance between the pump and the water level is $H = 3m$. Furthermore, the total friction loss in the inlet pipe, the water temperature and the barometric pressure as well as the $NPSH_R$ are given below:

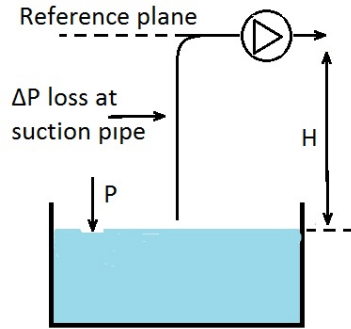


FIGURE 4.3: Sketch of an hydraulic system comprised an open tank and pump.

Water temperature = $40^\circ C$

Barometric pressure = $101.3kPa$

Pressure loss in the suction line at the present flow = $3.5kPa$

$NPSH_R = 4m$

The vapor pressure of the water at the temperature of $40^\circ C$ can be found in the table of "Physical properties of water" (see appendix A). Thus, at water temperature of $40^\circ C$, the vapor pressure is $7.37kPa$ and $\rho = 992.2 \frac{kg}{m^3}$. For this system, the equation 4.1 can be written as:

$$NPSH_A = \frac{(p_{barom} + \rho g H - \Delta p_{loss, \text{suct. pipe}}) - p_{vapour}}{\rho g} [m] \quad (4.6)$$

At this point it is worth nothing that the water's level vertical position is placed below the pump. Thus, H is negative. The system $NPSH_A$ value is:

$$NPSH_A = \frac{101300Pa}{992.2 \frac{kg}{m^3} 9.81 \frac{m}{sec^2}} - 3m - \frac{3500Pa}{992.2 \frac{kg}{m^3} 9.81 \frac{m}{sec^2}} - \frac{7375Pa}{992.2 \frac{kg}{m^3} 9.81 \frac{m}{sec^2}},$$

$$NPSH_A = 6.3m,$$

$$6.3 > 4 \implies NPSH_A > NPSH_R$$

4.2 Consideration of ship's stability and trim

A tanker operates within a comprehensive scheme of international standards set by the International Maritime Organization [16]. Therefore, the International convention for the prevention of pollution from ships (MARPOL)[17] sets strict standards in order to prevent ship-generated pollution. In addition, the International convention on load lines [18] determines the limitations on the draught to which a ship may be loaded. Furthermore, the International convention for the safety of life at sea (SOLAS) [19] specifies standards concerning the safety of merchant vessels.

A new building is accompanied by its unique “Trim and Stability booklet” which contains all the stability calculations for the intact and damaged states of the vessel [20] in compliance with the international regulations. In this context, the model is taking into consideration all necessary information needed for the stability and trim calculations from the “Trim and Stability Booklet” of an existing ship. Thus, the following steps were followed for the calculation of model's trim and draught:

1. x-moments and z-moments are derived from the calculated masses of each cargo and ballast tank multiplied by their corresponding longitudinal center of gravity (LCG) and vertical center of gravity (VCG) respectively. The measure of each tank weight is accomplished by deducting discharged volume (in both cargo and ballast systems) and utilizing the “Tank calibration tables” (see table 4.1) of the ship.

TABLE 4.1: The calibration table of No.2 portside Cargo Oil Tank, as presented in the “Trim and stability booklet” of Aframax tanker.

TANK CALIBRATION TABLE					
Tank name:	C.O.T. 2 (P)				
level from bottom (m)	volume (m^3)	lcg (m)	vcg (m)	tcg (m)	inertia moment (m^4)
0.4	188.93	61.192	2.519	-7.923	10250
2	984.09	61.195	3.335	-8.261	13007
4	2061.4	61.202	4.377	-8.667	15662
6	3160.92	61.211	5.4	-8.86	15662
8	4260.44	61.216	6.411	-8.953	15662
10	5359.97	61.218	7.418	-9.008	15662
12	6459.49	61.22	8.422	-9.044	15662
14	7559.01	61.221	9.425	-9.07	15662
16	8658.54	61.222	10.427	-9.089	15662
18	9758.06	61.223	11.429	-9.104	15662
19.731	10456.78	61.224	12.068	-9.037	0

The procedure indicated above, is repeated for each cargo and ballast tank at regular time intervals during the simulation in order to calculate the displacement, LCG and VCG of the ship. The calculations of a random time step are presented in table 4.2.

TABLE 4.2: Values of displacement, LCG and VCG, as calculated by the present model at a random time step.

	mass (tons)	LCG (m)	x-moment	VCG (m)	z-moment
LS and other	2541.5	-84.87	-215697.1	14.9	37868.35
CARGO 1P	6243.9	89.4	558400.6	10.1	63246.6
CARGO 1S	6242.6	89.43	558281.1	10.13	63223.5
CARGO 2P	8135.8	61.22	498087.3	9.95	80956.7
CARGO 2S	8137.1	61.22	498168.6	9.95	80979.7
CARGO 3P	7761.5	31.30	242933.4	9.58	74344.7
CARGO 3S	7786.8	31.30	243726.3	9.60	74766.7
CARGO 4P	6669.1	1.34	8936.6	8.59	57256.7
CARGO 4S	6673.2	1.34	8942.1	8.59	57317.0
CARGO 5P	7397.2	-28.62	-211706.6	9.25	68404.7
CARGO 5S	7432.1	-28.62	-212708.0	9.28	68964.8
CARGO 6P	5698.8	-55.20	-314563.4	9.85	56110.5
CARGO 6S	5700.1	-55.20	-314631.8	9.85	56130.8
CARGO SLOP P	0.0	-69.77	0.0	2.33	0.0
CARGO SLOP S	0.0	-69.77	0.0	2.33	0.0
BALLAST 1P	3.4	88.02	300.4	0.05	0.2
BALLAST 1S	3.4	88.02	300.4	0.05	0.2
BALLAST 2P	5.7	60.71	345.1	0.02	0.1
BALLAST 2S	5.7	60.71	345.1	0.02	0.1
BALLAST 3P	6.3	31.30	195.7	0.01	0.1
BALLAST 3S	6.3	31.30	195.7	0.01	0.1
BALLAST 4P	7.5	1.34	10.0	0.01	0.1
BALLAST 4S	7.5	1.34	10.0	0.01	0.1
BALLAST 5P	9.2	-28.01	-257.9	0.02	0.2
BALLAST 5S	9.3	-28.00	-259.9	0.02	0.1
BALLAST 6P	11.6	-56.00	-647.3	0.05	0.6
BALLAST 6S	11.6	-56.00	-647.3	0.05	0.6
BALLAST FPT	2.6	109.61	283.8	0.15	0.4
TOTAL	86509.8 tons	14.97	37554685.4	9.39	23562383.8

2. Then, taking into account vessel's equilibrium, by using the calculated displacement and utilizing the "Hydrostatic tables", a draught can be obtained. This draught (T_{LCF}), is the draught at the LCF location which remains constant at any possible trim condition for the same displacement. In the "Hydrostatic tables" at this LCF draught, the moment to trim MCT (Moment to change Trim per one Centimeter), the LCB (Longitudinal Center of Buoyancy) and LCF (Longitudinal Center of Floatation), are obtained.
3. Thereafter, the tangent of the ship's rotational angle θ (as shown in figure 4.4) can be calculated as follows:

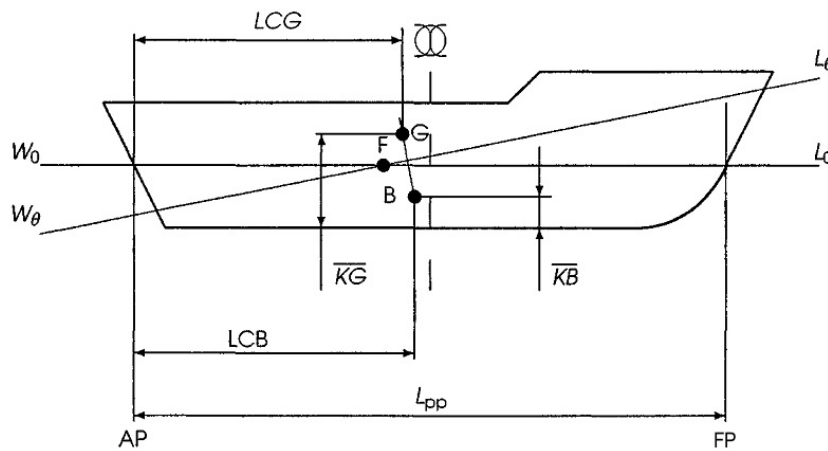


FIGURE 4.4: Trim and draught calculation.

$$\tan(\theta) = \frac{\text{Displacement}(LCG - LCB)}{L_{BP}MCT} \quad (4.7)$$

4. Furthermore, the draughts along the waterline can be calculated as follows:

$$T = T_{LCF} + (x - LCF) \tan(\theta) \quad (4.8)$$

where, x is assumed as the distance from the after peak (i.e. the origin is set at the after peak).

Thus, the after and forward draughts can be obtained as:

$$T_F = T_{LCF} + (L_{BP} - LCF) \tan(\theta) \quad (4.9)$$

$$T_A = T_{LCF} + (0 - LCF) \tan(\theta) \quad (4.10)$$

5. Finally, trim is defined as follows:

$$Trim = T_F - T_A \quad (4.11)$$

It is necessary to ascertain that when trim value is negative then it is assumed as trim by stern, otherwise it is assumed as trim by bow.

4.3 Shear Forces and Bending Moments

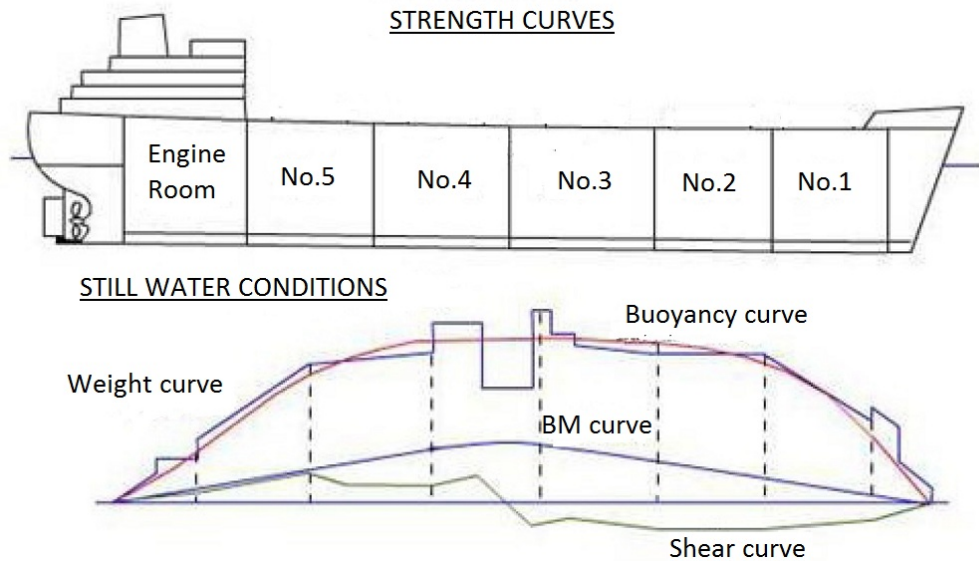


FIGURE 4.5: Strength curves in still water condition.

Over the years classification societies enact construction rules for the hull as well as for all important components of a ship, in order to ensure its safe operation and elongate its lifetime. In this context, is necessary to consider the negative effects that are produced by the shearing forces and bending moments which act upon a ship's structure. For instance, failures often occurs at welded joints as well as cracks and signs of corrosion in case of a continuous strain that effects on the particular section of the structure. In the present section, shear forces and bending moment calculations will be presented.

Shear stress is the force, F , acting on a given section divided by its cross sectional area, A . It is worth noting that the direction of the force F is considered as positive if is in the same direction as weight [21].

Bending moment is the force multiplied by the distance from a point of reference. Therefore, if the force is a point load, bending moment can be calculated as the force multiplied by the distance. In case of a distributed force, the bending moment is expressed as the integration of the distributed force multiplied by the distance.

Normally, shear forces and bending moments are tested in port and undersea state in order to determine the extent of permissible limits. In the present study the modeled ship discharges while set in port condition, so that the assumption of a ship floating in still water (harbor) will be followed. Thus, the modeled vessel can be considered as a homogeneous beam floating at rest, in still water.

The total load at any point of a homogeneous beam, is the difference between the downwards and the upwards forces, where the downward forces represent the weight of the ship and the upward forces represent the buoyancy, as shown in equation 4.12:

$$Load(x) = Weight(x) - Buoyancy(x) \quad (4.12)$$

Furthermore, shear forces distribution along the length of the ship, can be defined as the integral of the total load distribution (see equation 4.13). In addition, the integral of shear forces distribution results to bending moments distribution along the length of the ship (see equation 4.14).

$$ShearForce(x) = \int_0^x Load(x)dx \quad (4.13)$$

$$BendingMoment(x) = \int_0^x Load(x)x dx \quad (4.14)$$

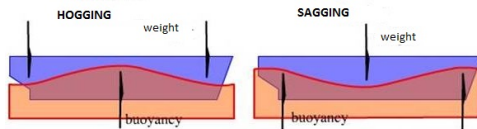


FIGURE 4.6: Hogging and Sagging.

While considering the tendency of a body to bend, the bending moment which measures this tendency, depends upon the amount of the acting load as well as the correlation between the load and the support method. Hence, distinction needs to be made between two different terms which describe bending moments, namely, hogging and sag-

ging. When a beam is subjected to external forces such that the beam bends with the ends curving downwards then it is termed as hogging stress. In the same way, when a beam is subjected to external forces such that the beam bends with the ends curving upwards then it is termed as sagging stress. Similarly, when a ship is loaded in such manner that a greater percentage of the load is around the amidship area then is sagging and in case of the greater percentage of the load located at the end holds, then is hogging (see figure 4.6) [22].

In the present study the calculation of bending moments and shear forces was accomplished by the following procedure:

- A diagram which represents the longitudinal distribution of weight and buoyancy as a function of ship's length was constructed. It is worth noting that the baseline (i.e. the length of the ship) is divided into a number of sections, as necessary, in order the distribution to be detailed enough. As a result, it can be assumed that the weight is evenly distributed between successive ordinates.

- As far as the weight distribution is concerned, it is assumed that the ship weight is divided in two main groups. The first weight group contains the Light Ship and the bunkering condition and remains constant during the simulation. While the second weight group contains the tank weights which are depended on the simulation time:

$$ShipWeight = (LightShip + BunkeringCondition) + (TanksVolumes) \quad (4.15)$$

- The first group of weights is taken from the “Trim and Stability Booklet”, as shown in tables 4.3 and 4.4 and the second group is calculated during the simulation (see section 4.2).
- Furthermore, the buoyancy distribution is calculated by using the Bonjean curves, which gives the immersed area of transverse sections to any given draft.
- Finally, the total load curve can be determined from the difference between weight and buoyancy of each section throughout the length of the ship. An excess of weight over buoyancy is considered to produce a positive load, whilst an excess of buoyancy over weight is considered to produce a negative load.

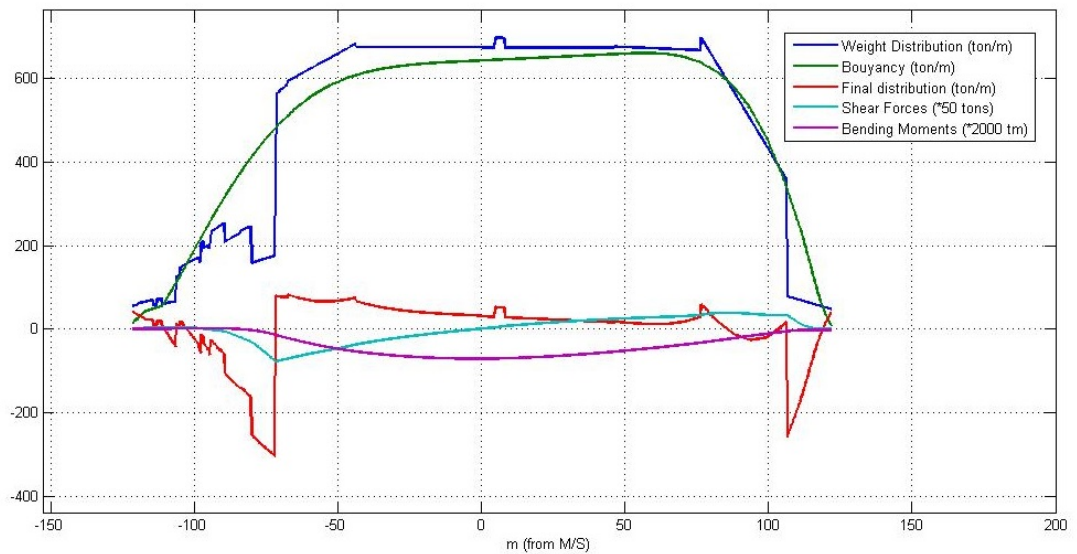


FIGURE 4.7: Results of strength calculation as per the present model.

To this end, shear forces and bending moments at any section of the ship can be determined from the load curve. Strength calculations at a random time as derived from Matlab, are presented in figure 4.7.

TABLE 4.3: Light Ship Distribution Data.

AFT. from M/S (m)	FWD. from M/S (m)	section weight (t)	LCG from M/S
-121.5	-106.6	585	-113.5
-106.6	-80.2	1920	-92.1
-80.2	-41.8	2387	-60.8
-41.8	76.6	7590	17.4
76.6	106.2	1623	90.6
106.2	122	735	113.5
-94.6	-80.2	357	-87.4
-106.6	-97	153	-101.8
106.2	122	196	113
-121.5	-106.6	121	-113.8
4.7	7.9	75	6.3
-91.4	-81.8	20	-86.6
-80.2	106.2	195	13
-84.2	106.2	768	6.4
-121.5	122	21	0
-94.6	-80.2	181	-87.4
-97.8	-89.8	358	-93.8
-111.4	-98.6	28.8	-105
-113	-111.4	25.8	-112.2
-105	-95.4	70.5	-100.2
-120	-114	19	-117
-105	-98.6	67.8	-101.8
-106.6	-80.2	270	-93.4
-106.6	-80.2	205	-93.4
-121.5	122	140	-25.1
-121.5	-114.6	86	-118
-121.5	-106.6	75	-113.8
-121.5	122	296	29.2
-121.5	122	292.9	29.2

TABLE 4.4: Bunkering condition.

Tank No.	AFT. from M/S (m)	FWD. from M/S (m)	Weight (t)	LCG from M/S
L.S.H.F.O.T 1 (P)	-80.2	-72	496.9	-76.1
H.F.O.T 1 (S)	-80.2	-72	0	-76.016
H.F.O.T 2 (P)	-97	-72	396	-87.868
H.F.O.T 2 (S)	-97	-72	640.2	-87.409
HFO SETT.T (P)	-83.4	-80.2	74.4	-81.8
HFO SERV.T (P)	-86.6	-83.4	74.4	-85
L.S.H.F.O.SETT.T (P)	-97	-91.4	47.9	-93.876
L.S.H.F.O.SERV.T (P)	-91.4	-78.56	61.6	-88.972
M.D.O.STOR.T(P)	-98.6	-87.4	24.7	-91.68
M.D.O.STOR.T(S)	-98.6	-84.2	42.1	-88.8
M.D.O.SERV.T(P)	-80.2	-77.74	29.3	-78.97
MAIN L.O.STOR.T.	-103.4	-100.2	31.5	-102.37
MAIN L.O SUMP.T.	-98.6	-89.8	22.8	-94.37
MAIN L.O SETT.T.(P)	-101.8	-100.2	0	-100.129
CYL.O.STOR.T.(P)	-105	-97	100.6	-100.13
G/E L.O. STOR. T.(P)	-105	-103.4	22.5	-104.2
CYL.O.STOR.T. LSHFO	-100.2	-97	27	-98.6
F.W.T. (P)	-111.4	-106.6	83.8	-108.88
D.W.T CONST. HALF	-85.8	-81	99.3	-84.76

Chapter 5

The development of the model at Matlab's Simulink environment

5.1 Matlab's Simulink environment

The model was developed in Matlab's Simulink environment. Simulink is a graphical extension to Matlab for modeling and simulation of systems. Matlab's Simulink is often used in simulation tests and that is because of the following advantages:

- An appreciably simplified procedure for the model development, exonerates the user from textual programming for the basic components. The model is represented graphically in Simulink as block diagrams. A wide array of blocks is available to the user in provided libraries, for representing various phenomena and models in a range of formats. Moreover, the model itself is the design flowchart.
- The developed subsystems can be generic and re-useable . There is a possibility of storing them in the topic-related libraries so as to be used in other systems.
- There is no need for making a program solving the system of equations of the mathematical model adopted, since there is a possibility of an easy selection of the method for solving the differential equations and determining the basic simulation parameters, such as the solver method, duration of the simulation, time step and precision of the results.
- A relatively short simulation time due to rapid and effective calculating algorithms is determined.

- A relatively easy change of the coefficients of the mathematical model, enabling an examination of the effect of the operational parameters upon the properties of the examined system.
- There are many computational advantages, such as memory management blocks for sparse matrices which can lead to dramatic improvements in execution time for programs working with large amounts of sparse data.

Developed model

The model consists of two basic subsystems, namely, the hydraulic and the system, which calculates the response of the ship. The latter one is fully parametric. In addition, the latter subsystem can be decoupled and used as an independent system for all stability and strength calculations, at any loading condition in still water. It is necessary to ascertain that the continuous monitoring of the static and dynamic loads of a ship's structure throughout its service life, is crucial. Moreover, all basic parameters are imposed in the model from external files (i.e. Excel and Matlab files). Therefore, the calculation of another vessel's response can be implemented, by simply substituting the above mentioned files, in the same format. The external files are listed below:

- Tank Calibration Tables
- Hydrostatic Tables
- Bonjean Curves
- Light Ship Distribution data table
- Bunkering Condition
- Basic Particulars of the vessel (L,B,T,D etc.)

As far as the ship's hydraulic system is concerned, all data are imported in such a way that the hydraulic cargo and ballast systems to be adapted for any other vessel. Thus, the characteristic curves of the pumps, the tank dimensions and the characteristic curves of boilers can be easily replaced with the corresponding ones of the new vessel. Nonetheless, the piping system arrangement should be modeled again, since piping arrangement differs for any other vessel. Consequently, the hydraulic model cannot be fully parameterized.

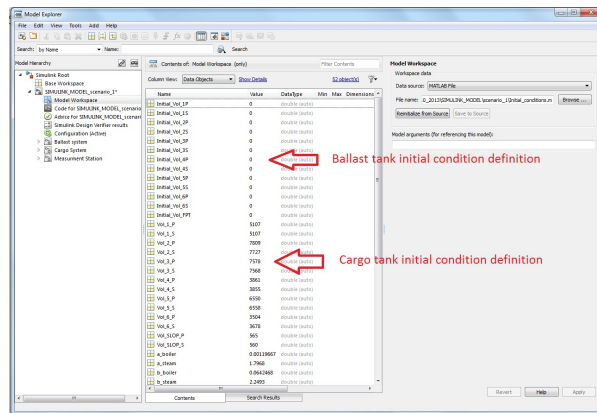


FIGURE 5.1: Model explorer user interface.

At this point, it should be noted that all model variables can be easily modified by the “Model explorer” tool, located at Simulink’s environment. The “Model explorer” tool (see figure 5.1), is a handy user’s interface and provides several options for each one of the components without the necessity of navigation through the model block diagram. In this context, all variables, which define any discharging scenario, are inserted in its workspace in order to be checked or changed easily. The variables which are necessary for the determination of each discharging scenario are listed below:

- Initial loading condition
- Shore system characteristics
- Number of pumps in use and their rotational speed
- Number of manifolds in use
- Cargo characteristic data

Vessel's basic characteristics

The modelling concerns the cargo and ballast systems corresponding to an existing Aframax tanker. The vessel's main technical characteristics are listed in table 5.1:

TABLE 5.1: Basic particulars of the Aframax tanker.

Ship Particulars	
Length:	234m
Breadth:	42m
Depth:	21m
Draught:	13.6m
DWT:	105,000ton
Ballast pump nominal characteristics	
Head:	25m
Flow Rate:	$1800 \frac{m^3}{hr}$
N:	1180rpm
Cargo pump nominal characteristics	
Head:	130m
Flow Rate:	$3000 \frac{m^3}{hr}$
N:	1330rpm

The tanker is double hulled with 6 pairs of cargo tanks and a pair of slop tanks. There are 3 manifolds, 3 steam driven cargo pumps and 2 electric driven ballast pumps. The pumps, which are located at the pump room, are connected with the cargo and ballast tanks via the piping network. A simplified piping diagram of the cargo (figure 5.2) and ballast (figure 5.4) system is presented below:

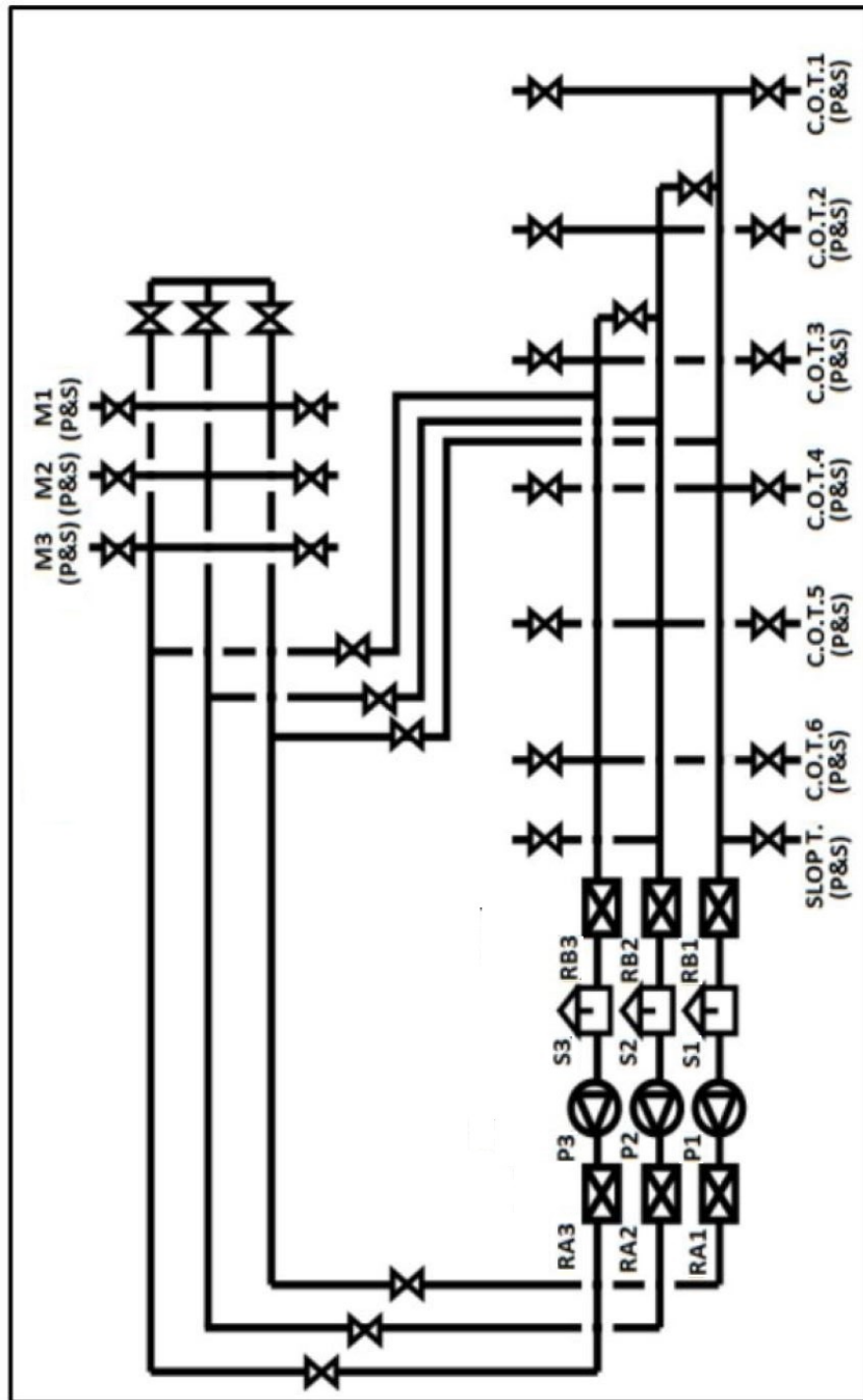


FIGURE 5.2: Simplified Cargo Piping Diagram of the Aframax tanker [23].







SYMBOL	DESCRIPTION
	Pump (P)
	Valve
	Separator Tank (S)
	Local Added Resistance (RA,RB)
	Box Type Strainer (ST)
	Sea Chest
M	Manifold
SLOP T.	Slop Tank
C.O.T.	Cargo Oil Tank
W.B.T.	Water Ballast Tank
P&S	Port & Starboard

FIGURE 5.3: Symbol description [23].

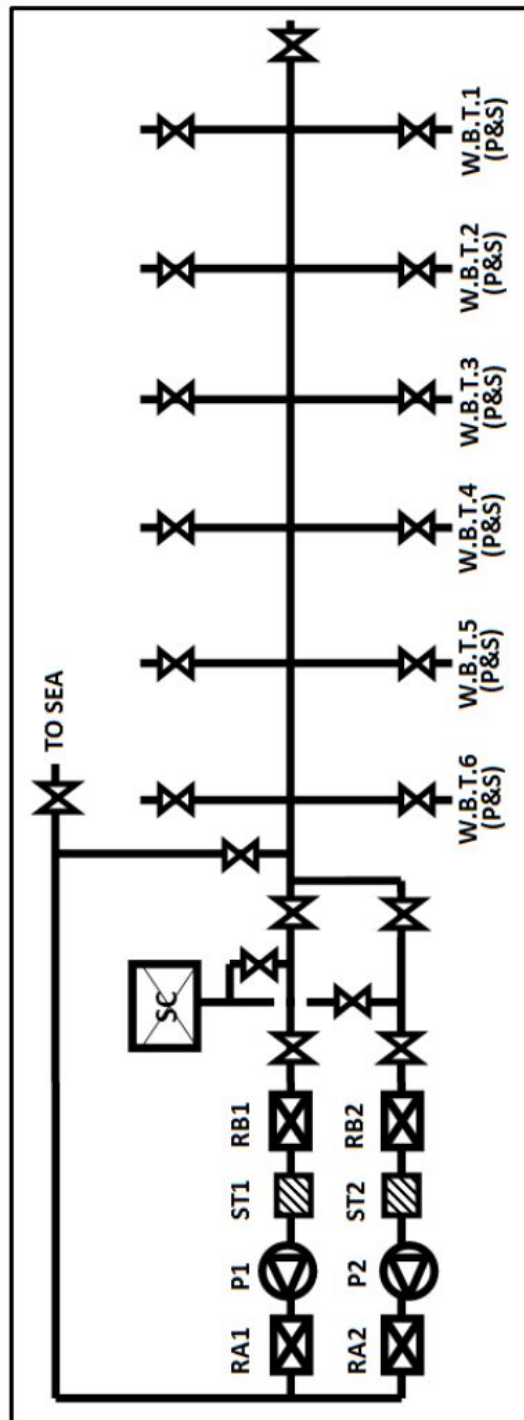


FIGURE 5.4: Simplified Ballast Piping Diagram of the Aframax tanker [23].

The vessel has the capability of simultaneously discharging 3 grades or types of cargo. Cargo is discharged at the manifolds, located amidships. Furthermore, all the tanks are connected to the manifolds via the piping network.

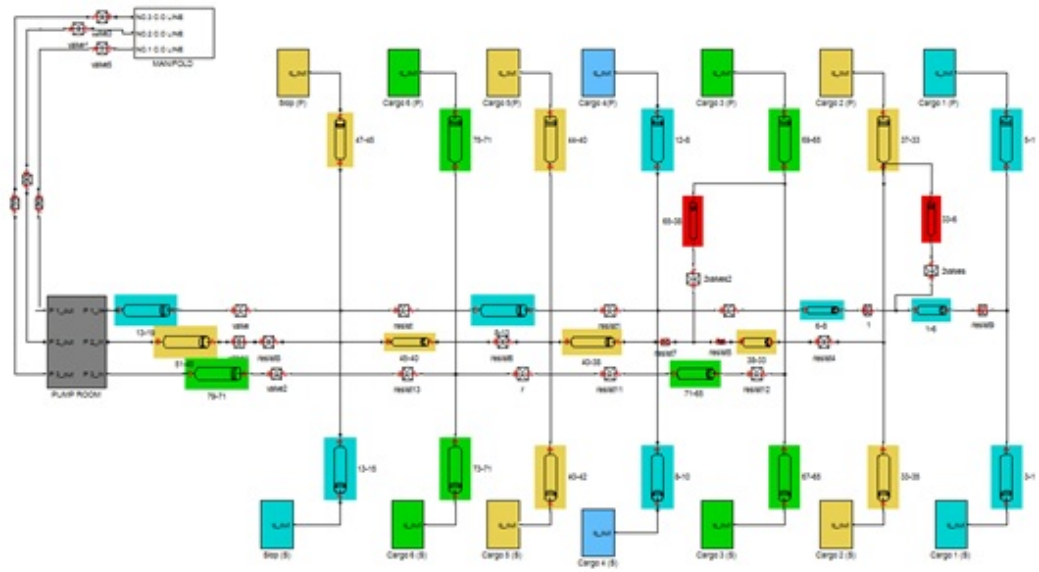


FIGURE 5.5: Sketch of cargo piping system of Aframax tanker. The cargo piping system consists of three segregated pipe lines including cross-over valves, as illustrated by different colors (yellow, green, blue, red).

5.2 The cargo and ballast model

The cargo and ballast systems are governed by the same hydraulic principles (see chapter 3). In addition, the cargo system consists of the cargo tanks, the three steam driven cargo pumps located at the ship's pump room and the manifolds. As far as the ballast system is concerned, it consists of the ballast tanks, the two electric driven pumps located at the ship's pump room and the inlet sea chests. Furthermore, the model takes into consideration the friction losses due to pipes, corners, valves or fittings (see section 3.6). The basic components of the hydraulic model will be analyzed in the sections below.

5.2.1 Modeling the tanks

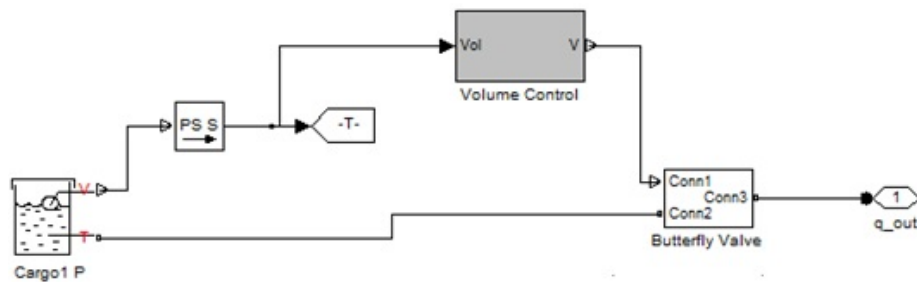


FIGURE 5.6: Cargo oil tank: In Matlab's Simulink environment, the subsystem consists of a pressurized tank, a volume control subsystem and a butterfly valve.

Each tank subsystem represents a pressurized tank in which fluid is stored under a specified pressure which remains constant throughout the procedure. For a tanker vessel, this means that in case of the cargo tanks the pressure equals to the inert gas pressure and in case of the ballast tanks the pressure equals to the atmospheric pressure. During the simulation, the volume of each tank is continuously measured for the following two main purposes:

- For the determination of the fluid level changes by utilizing the “Tank volume tables”, which represent the correlation between fluid level and volume of each tank. The “Tank volume tables” can be found at the “Trim and Stability Booklet”, as prescribed in section 4.2.
- For the application of automatic control to the butterfly valve which is placed in the inlet of each tank. Thus, when a cargo tank volume decreases to zero, the valve at

the inlet of this tank closes. Similarly, in the ballast system, when a tank fills, the valve closes automatically in order to avoid overflow. It is worth noting that at the beginning of the simulation all valves are opened with respect to the discharging scenario.

To this end, the mathematical equations which describe the main hydraulic characteristic values of the tank subsystem are presented below:

The pressure at the tank inlet is calculated as follows:

$$p = p_{elev} - p_{loss} + p_{pr} \quad (5.1)$$

where:

$$p_{elev} = \rho g H \quad (5.2)$$

$$p_{loss} = K \frac{\rho}{2A_p^2} q |q| \quad (5.3)$$

Where,

$$A_p = \frac{\pi d^2}{4} \quad (5.4)$$

And the instantaneous fluid volume of each tank is given by:

$$V = V_0 - qt \quad (5.5)$$

where:

p Pressure at the tank inlet

p_{elev} Pressure due to fluid level

p_{loss} Pressure loss in the connecting pipe

p_{pr} Pressurization

ρ Fluid density

g Acceleration of gravity

H Fluid level with respect to the bottom of the tank, which is specified as $H = f(V)$

K Pressure loss coefficient

A_p Connecting pipe area

d Connecting pipe diameter

q Flow rate

V_0 Initial fluid volume

A Tank cross-sectional area

t Simulation time

5.2.2 Modeling the pumps

The pumps (cargo and ballast) are located in the pump room. The pump room is a separate room in the ship for pumping equipment, located between the engine room and the cargo hold. The vessel is equipped with 3 steam cargo pumps and 2 electrical driven ballast pumps.

The pump room is consisted of five independent pump subsystems, so that the three refers to the cargo pumps and the two to the ballast pumps. Furthermore, each pump subsystem, is consisted of an angular velocity source, a pump, valves and fittings (such as separator tank, flow meters e.t.c.) with respect to the ship cargo and ballast piping diagrams (see figure 5.7). It is worth noting that the angular velocity source is a parametric value and can be either a constant value or a time dependent variable. The angular velocity can be defined by the user at the beginning of the simulation.

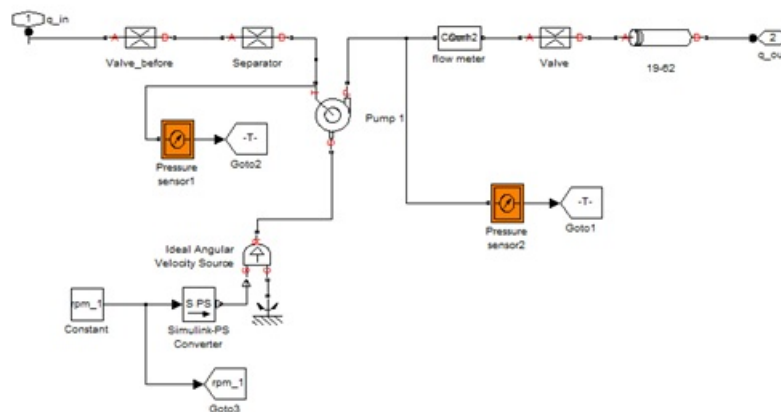


FIGURE 5.7: Cargo oil pump: In Matlab’s Simulink environment, the subsystem consists of a centrifugal pump, sensors and valves.

The pump room and the cargo and ballast piping diagrams have been visualized by using a visualization routine developed in Rhinoceros software as presented in figure 5.8 [23].

All pumps are centrifugal pumps and they modeled as a data sheet-based model. Their characteristic curves are given by the manufacturer. Each pump is parameterized by pressure differential and power consumption vs. pump delivery characteristics. The pump characteristics are calculated by using two one-dimensional table lookups: for the head (pressure) based on the pump flow rate and for the pump power consumption based on the pump flow rate given by the manufacturer. Both characteristics are specified at

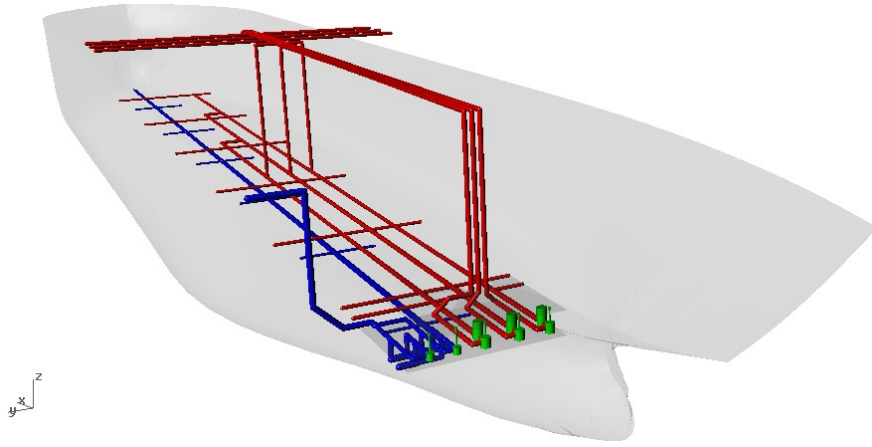


FIGURE 5.8: Model of cargo (red) and ballast (blue) piping system [23].

the same angular velocity ω_{ref} (Reference angular velocity) and the same fluid density ρ_{ref} (Reference density).

It is necessary to ascertain that the calculation of head (pressure) at another angular velocity or for any other liquid (different density) is expressed by the affinity rules (see section 3.1) in order to redefine the characteristic curves. Thus, the new flow rate q can be calculated as follows:

$$q = q_{ref} \frac{\omega}{\omega_{ref}} \quad (5.6)$$

Moreover, the head across the pump at current angular velocity ω and density ρ is calculated as:

$$H = H_{ref} \left(\frac{\omega}{\omega_{ref}} \right)^2 \frac{\rho}{\rho_{ref}} \quad (5.7)$$

where H_{ref} is determined from the $H - Q$ characteristic curve of the existing pump, which refers to the nominal angular velocity ω_{ref} and density ρ_{ref} of the reference liquid (i.e. the pumped liquid during the pump tests as recorded by the manufacturer). The equation which determines the pump's power consumption is:

$$P = P_{ref} \left(\frac{\omega}{\omega_{ref}} \right)^3 \frac{\rho}{\rho_{ref}} \quad (5.8)$$

where P_{ref} is the reference power consumption obtained from the $P - Q$ characteristic curve.

5.2.3 Modeling the pipes, valves and fittings

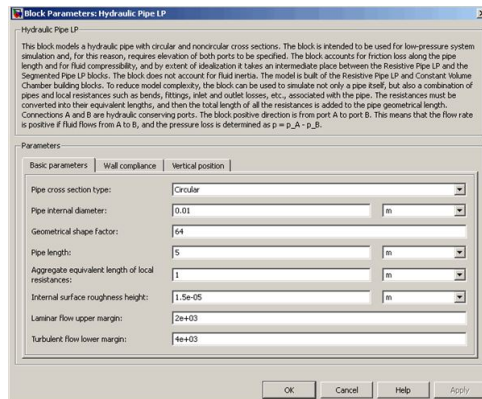


FIGURE 5.9: Pipe user interface for setting the parameters of interest.

reduce model complexity. The resistances must be converted into their equivalent lengths (see section 3.6), and then the sum of all equivalent lengths is added to the pipe geometrical length. The basic parameters which are needed to be defined in Simulink are:

- **Pipe cross section type**
- **Pipe internal diameter**
- **Pipe length**
- **Aggregate equivalent length of local resistances**
- **Internal surface roughness**
- **Laminar flow upper margin and Turbulent flow lower margin**
- **Pipe wall type (rigid or flexible)**
- **Vertical position of the pipe**

As far as the piping elements (i.e. connections, fittings, valves, elbows etc.) are concerned the local resistance block is utilized. The basic block parameters which are needed to be defined in Simulink are:

In the present study, all pipes, valves and fittings are modeled according to the available pipe diagrams of the vessel (see figures 5.2, 5.4).

As far as the piping network is concerned, the Hydraulic Pipe LP block (see figure 5.9), which is available in Simulink’s hydraulic library, models hydraulic pipelines with circular and non circular cross sections. The block takes into consideration the friction loss along the pipe length. In addition, the block can be used to simulate not only a pipe itself, but also a combination of pipes and local resistances, such as bends, fittings etc. associated with the pipe, in order to

·**The resistance area**

·**The pressure loss coefficient**

There are two different methods for the specification of the pressure loss coefficient, namely, by semi-empirical formulas and by tabulated data which contains the loss coefficients as a function of the Reynolds number (see section 3.6). The pressure coefficients are usually provided in catalogs, data sheets, or hydraulic textbooks by the manufacturer.

5.2.4 Cargo (crude oil) definition in the model

The cargo system has the capability of simultaneously offloading 3 different types of cargo while ballasting sea water. In this context, four different fluid blocks were connected to the model. For every fluid block, the following parameters should be defined:

- **Fluid density**
- **Kinematic viscosity**

It is important to point out that regarding crude oils, usually the following data are provided by the petroleum industries:

- **Crude oil name**
- **API gravity**
- **Reid vapor pressure**
- **Kinematic viscosity at a specific temperature**

Thereafter, the density of a crude oil is implicitly defined from its API gravity. The American Petroleum Institute gravity, or API gravity [24], is a measure of how heavy or light a petroleum liquid is compared to water. Thus, a value of API gravity greater than 10, results in lighter petroleum which floats on water, else is heavier and sinks. Although API gravity has no units, it is referred to as being in “degrees”. The density of petroleum liquids can be obtained from API gravity, as follows:

Firstly, the specific gravity is calculated as:

$$SG_{at60^{\circ}F} = \frac{141.5}{APIgravity + 131.5} \quad (5.9)$$

Then, the density of the crude oil is derived as:

$$\rho_{oil} = SG_{oil} \cdot \rho_{H_2O} \quad (5.10)$$

5.3 Measurement station

The independent subsystem, namely “Measurement Station”, which has been developed, generates the interaction of the hydraulic system and ship’s response. The continuous calculations of the hydraulic model (output) is used as input (i.e. loading condition) to the “Measurement Station” independent system for the stability and strength calculations. Thus, although the hydraulic calculations are continuous, a periodically calculation of ship’s response (i.e. stability and strength) ensures that the selected discharging plan (initial conditions) is implemented with respect to the acceptable stability and strength limits.

Furthermore, the final output files of the model, namely the “Pumping Log” and the “Oil Transfer Plan”, summarizes all critical hydraulic calculations during the simulation and its corresponding hydrostatic, strength values and fuel consumption for further analysis. It is worth noting that the configuration of the output was chosen in respect to the existing recorded files of relevant procedures provided by the operator. The final output files of the model will be analyzed in section 5.3.1 and the basic flow chart of the stability and strength calculation during the discharging procedure will be presented in section 5.3.2.

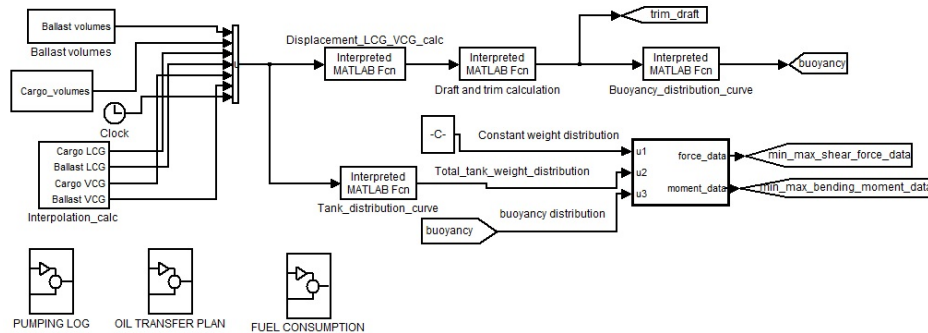


FIGURE 5.10: Measurement Station subsystem, as shown in Matlab’s Simulink environment.

5.3.1 Pumping log and Oil Transfer Plan

An accurate log shall be maintained regarding the discharge operation. In this context, two different logs are kept, namely the “Pumping Log” and the “Oil Transfer Plan”. Pump operation in practice, is extremely complex, so that during an actual discharging operation, the reason of every stoppage or change (e.g. rpm of each pump, times of

starting and finishing individual cargo tanks) is recorded to the relative “Pumping Log”. As a matter of fact, it is very important to record the times and reason for any delay or stoppage. Furthermore, it should be recorded the party or equipment responsible for the stoppage and whether the stop was ordered by the ship or shore too. In this manner, if an incident occurs during the discharging, all relative records are at the disposal of the authorities.

As far as the “Oil Transfer Plan” is concerned, all further information regarding the discharging procedure, such as the loading condition, the corresponding mean draft, trim, maximum shear forces, bending moments and energy consumption are being kept. All ships are designed with limitations imposed upon their operability to ensure that their structural integrity is maintained. Thus, it is important to load the cargo so that stresses in the ship remain at a minimum level. Therefore, exceeding these limitations may result in over-stressing of the ship’s structure which may lead to catastrophic failure. So, all calculations in still water of shear forces and bending moments will be provided, for any loading condition.

In recent years the industry adopted fuel energy saving practices on account of the steep increase of fuel (bunker) prices. In this context the fuel consumption was calculated and recorded in the “Oil Transfer Plan” in order to focus on the energy efficiency of cargo pumping systems. The output forms of the “Pumping Log” and “Oil Transfer Plan” which are being produced every one hour, are shown in figures 5.2 and 5.3 respectively.

TABLE 5.3: Oil transfer plan

Oil Transfer Plan					
TIME					
Total Bbls					
Total M/T CARGO(Bbls)					
Total M/T Ballast(Bbls)					
Draft F					
Draft A					
TRIM					
Max shear force					
Max bending moment					
Tank No(Bbls)					
CARGO 1P					
CARGO 1S					
CARGO 2P					
CARGO 2S					
CARGO 3P					
CARGO 3S					
CARGO 4P					
CARGO 4S					
CARGO 5P					
CARGO 5S					
CARGO 6P					
CARGO 6S					
CARGO SLOP P					
CARGO SLOP S					
BALLAST 1P					
BALLAST 1S					
BALLAST 2P					
BALLAST 2S					
BALLAST 3P					
BALLAST 3S					
BALLAST 4P					
BALLAST 4S					
BALLAST 5P					
BALLAST 5S					
BALLAST 6P					
BALLAST 6S					
BALLAST FPT					
Fuel consumption					

5.3.2 Ship's stability and strength calculations

A ship's structure is designed to withstand the static and dynamic loads likely to be experienced throughout its service life. The ship's response (i.e. stability and strength calculations), is implemented in the "Measurement Station" subsystem.

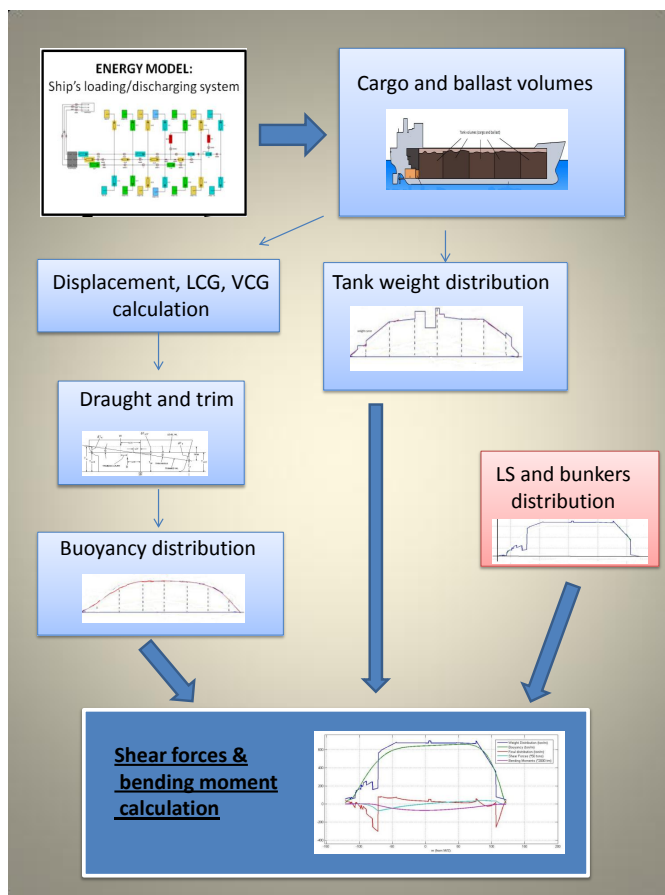


FIGURE 5.11: Flow chart of stability and stress calculations every time step.

bending moment distribution curves are derived.

It is worth noting that in figure 5.11, all components colored in blue, are time depended variables. The user, at the beginning of the simulation, can define the time step in which the calculations will take place. A time step of 15 or 30 minutes is adequate to ensure that ship's response will be within the design limits. Moreover, the box colored in light red represents the light ship weight distribution, including the bunkers weight distribution, which remains constant during the simulation.

The flow chart in figure 5.11 represents the process as executed in Simulink:

Firstly, the time depended cargo and ballast volumes variables, which derive from the hydraulic model, are used for the calculation of the displacement, LCG, VCG and the tank weight distribution (see sections 4.2 and 4.3). Then, from the calculated displacement and LCG, the draught and trim are defined.

Thereafter, the buoyancy distribution curve is derived from the calculated trim and draught by utilizing the "Bonjean tables".

Subsequently, the total load distribution of the ship is calculated by adding the weight distribution and the buoyancy distribution curves.

Finally, the shear forces and

5.3.3 Energy calculation - Fuel oil consumption

The subsystem that calculates the fuel consumption is shown in figure: 5.12.

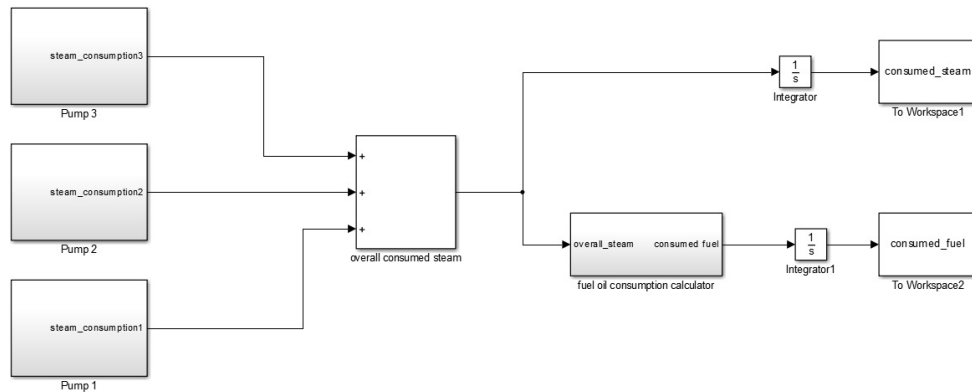


FIGURE 5.12: Boiler fuel consumption subsystem as illustrated in Matlab's Simulink environment.

The consumed steam at each pump, is calculated as follows:

The steam consumption ($\frac{Kg}{sec}$) in relation to Q ($\frac{m^3}{sec}$) at the nominal rpm (1350 rpm) is approximated by a first order polynomial (linear approximation) in the sense of least mean square, as shown in figure: 5.13. The approximated function provides the ability to calculate the steam consumption of the pump at any point in the range of Q .

$Q(m^3/h)$	Steam consumption(kg/h)
656	9249
1547	10861
2379	12498
3018	13505
3139	13671

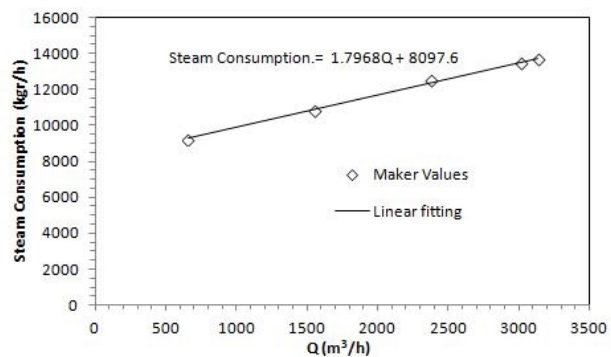


FIGURE 5.13: Steam consumption of cargo oil pump as function of consumed steam at nominal speed (1330rpm) given by the manufacturer.

Thus, the consumed steam at each pump can be derived from:

$$Q_{steam} = 1.7968Q_{pump} + 2.2493 \quad (5.11)$$

and the overall consumed steam of the system, during the discharging procedure is:

$$Q_{total} = Q_{pump1} + Q_{pump2} + Q_{pump3} \quad (5.12)$$

Subsequently, the fuel oil consumption to the boiler in relation to the steam consumption to the pumps is approximated by a second order polynomial in the sense of least mean square, as shown in figure: 5.14:

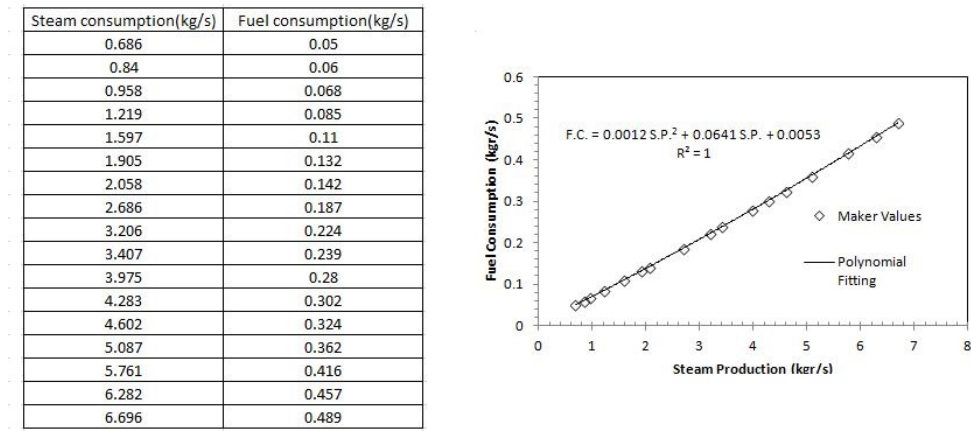


FIGURE 5.14: Fuel consumption of boiler as function of produced steam given by the manufacturer.

Finally, the fuel consumption at the boiler can be derived from the following equation:

$$FuelConsumption = 0.0012Q_{total}^2 + 0.0642Q_{total} + 0.0052 \quad (5.13)$$

5.4 Solver configuration

A solver is connected to the model in order to apply a numerical method to solve the set of ordinary differential equations which govern the hydraulic cargo and ballast models. A Matlab's Simulink solver should ensure the required accuracy of the simulation. Furthermore, the solver should accomplish the simulation in the shortest possible amount of time. In this context, the selection process of the appropriate solver, in order to satisfy the above mentioned parameters, is as shown in the flow chart 5.15 .

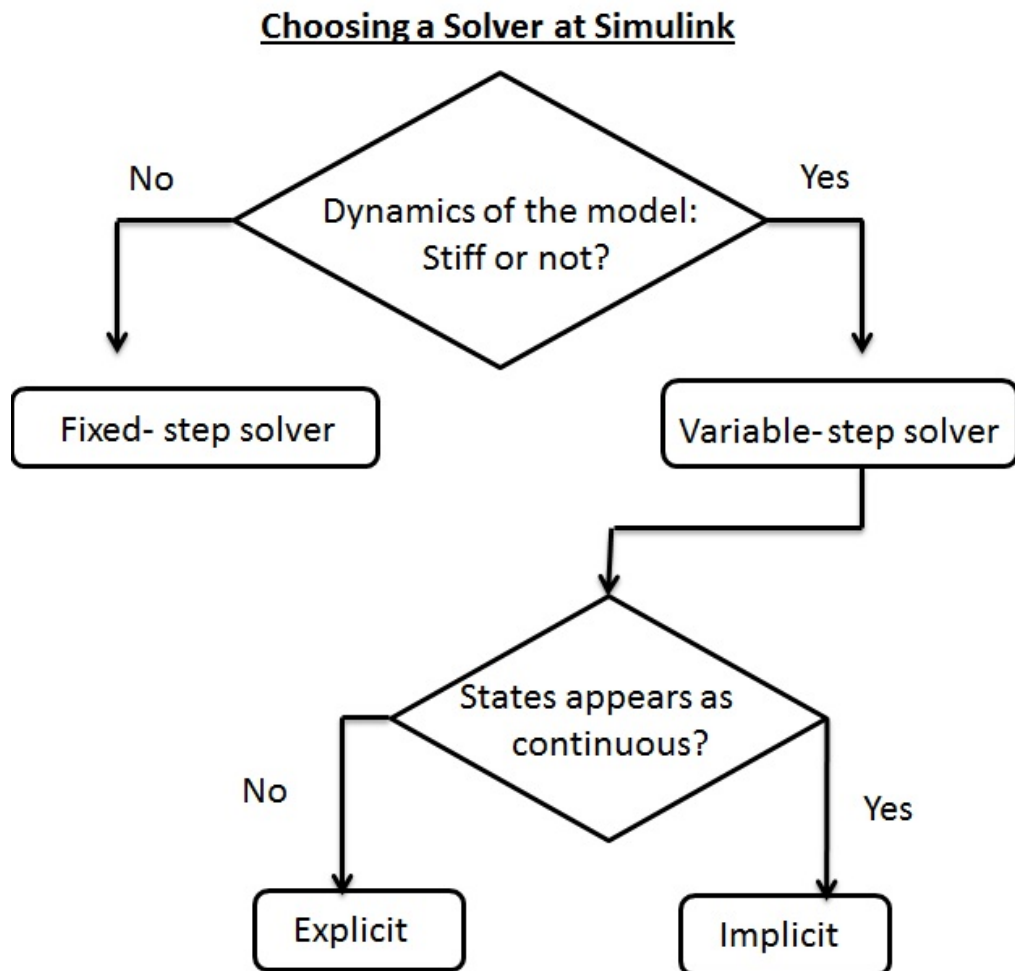


FIGURE 5.15: Decision tree for solver at Simulink.

Firstly, the solver type must be chosen between the two available types of solvers, namely, the fixed-step and variable-step. The fixed-step solver has a fixed time interval between the calculations which is called step size and remains constant throughout the simulation. The next simulation time is calculated as the sum of the current simulation time and the

step size. In the variable-step solver the step size can vary from one step to another in order to keep the simulation within the error tolerances that are specified. A variable-step solver might shorten the simulation time of the model significantly, since it can dynamically adjust the step size as necessary and hence reduce the number of steps needed, for a given level of accuracy. The choice between a variable-step and a fixed-step solver depends on the dynamics of the model, so that the variable step solver type was selected.

Secondly, the two choices of the variable-step solvers were concerned, namely, the implicit or explicit. The final decision depends on whether the blocks in the model define states or not, and if so, the type of states that they define. The model has continuous states, so that the use of numerical integration is needed in order to calculate the values of the continuous states at the next time step. For physical models, such as Simscape models, MathWorks recommends implicit solvers, since they require fewer time steps than explicit solvers. Finally, taking into consideration all the above constraints, the implicit variable-step solver 23t, was selected.

Finally, the solver parameters have to be specified, such as the simulation time, the error tolerances, the Jacobian method and the compiler. The simulation time is the duration of the modeled procedure. It is worth noting that, in case of the simulated procedure ends earlier than the defined simulation time, the simulation stops. Thus, if the simulation time has been set to 20hours and the vessel discharges all cargo within the first 16hours, then the simulation will stop earlier. The variable-step solvers use standard control techniques to monitor the local error at each time step. During each time step, the solvers compute the state values at the end of the step and determine the local error, thus the estimated error of these state values. Then, there is a comparison between the local error and the acceptable error in order to redefine the step size. Thus, if the local error is greater than the acceptable error for any one state, the solver reduces the step size. The acceptable error is a function of both the relative and absolute tolerance. The relative tolerance measures the error relative to the size of each state. The relative tolerance represents a percentage of the state value. The absolute tolerance is a threshold error value, which represents the acceptable error as the value of the measured state when approaches zero. In other words, for each i state, the following must be satisfied:

$$e_i \leq \max(\text{relativetolerance} * |x_i|, \text{absolutetolerance}_i) \quad (5.14)$$

where: e_i is the error for the i th state.

Figure 5.16 shows a plot of a state and the regions in which the relative tolerance and the absolute tolerance determine the acceptable error. For implicit solvers, Simulink must

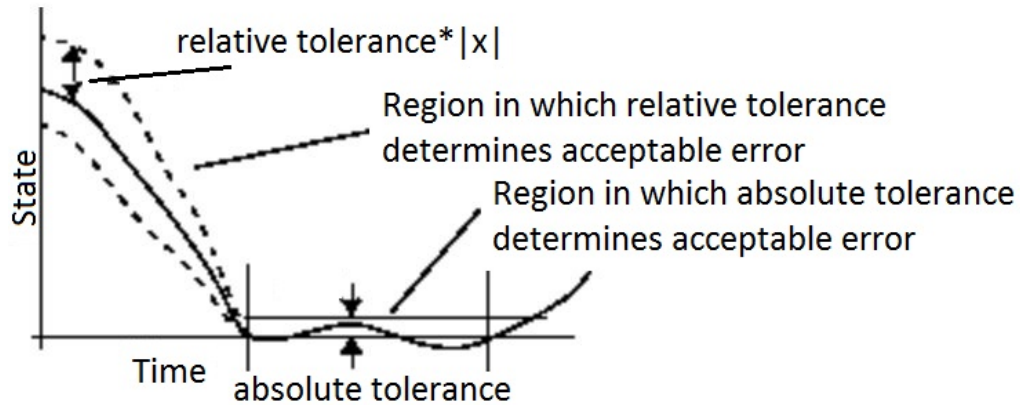


FIGURE 5.16: Graphical representation of relative and absolute tolerance determination.

compute the solver Jacobian, which is a submatrix of the Jacobian matrix associated with the continuous representation of a Simulink model. In general, this continuous representation is of the form:

$$\dot{x} = f(x, t, u) \quad (5.15)$$

$$y = g(x, t, u) \quad (5.16)$$

The Jacobian, J , formed from this system of equations is:

$$J = \begin{bmatrix} \frac{\partial f}{\partial x} & \frac{\partial f}{\partial u} \\ \frac{\partial g}{\partial x} & \frac{\partial g}{\partial u} \end{bmatrix}.$$

And the solver Jacobian is the submatrix J_x :

$$J_x = \frac{\partial f}{\partial x} \quad (5.17)$$

For any implicit solver, in the relative pane of the configuration parameters dialog box, a parameter called Solver Jacobian method and a drop-down menu appear (see figure 5.17). This menu has five options for computing the solver Jacobian: auto, Sparse perturbation, Full perturbation, Sparse analytical, and Full analytical. The full and sparse analytical methods attempt to improve performance by calculating the Jacobian using analytical equations rather than the perturbation equations. The sparse analytical method, also uses the sparsity information to accelerate the linear algebraic operations required to solve the ordinary differential equations.

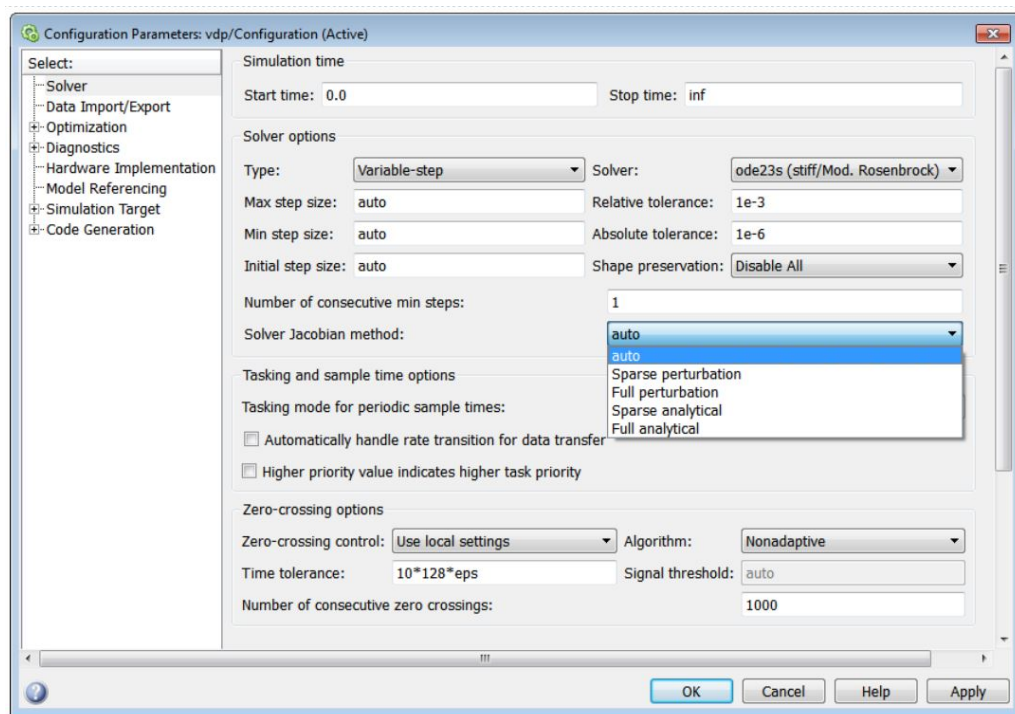


FIGURE 5.17: .

Chapter 6

Validation of the Model

The vessel's operator provided cargo discharge logs for a number of discharging operations at Baytown's terminal in Texas, USA (see figure 6.1). A number of cargo discharging procedures were simulated by utilizing the model. The parameters of the model were defined similarly as in the provided discharge logs and the validation was achieved by comparing the recorded with the calculated data.



FIGURE 6.1: Baytown tanker terminal in Texas (source: Google maps).

The simulation scenarios (case studies) defined with respect to the available pumping logs and oil transfer plans which derive from the actual discharging procedures. Namely, the initial loading condition of the cargo tanks, the discharged crude oil and the way of the discharging procedure was set similarly to the corresponding actual procedures. To

this end, the details of each case study regarding the above mentioned data are presented in sections 6.1, 6.2, 6.3.

For every discharging scenario the following assumptions were made:

- The ballast tanks at the beginning of the procedure are considered empty. The vessel's ballasting starts simultaneously with the cargo discharging procedure, using the two electric driven ballast pumps working at their nominal rotational speed (1180 rpm) and the respective valves fully open.
- For the shore line, a simplified approach was applied. It was assumed that the piping network consists of one pipe with length equal to that given by the shore officer, connected to the shore storage tanks. The diameter of those pipes is set to be 500A (0.5m). The dimensions of the shore tanks has not been provided, so that it was assumed to be of diameter 80m (i.e. the base area is $5026.4m^2$) and max height of 22 m. In the simulation model these parameters can be easily changed in order to reflect any given size of shore tank.

6.1 Case study 1

The initial loading conditions of the cargo tanks are presented in table 6.1. Two cargo pumps are used, working at the same rotational speed (1200rpm) . The cargo was discharged at the two of the three available manifolds. Thus, the involved piping network according to the discharging plan, is illustrated in figure 6.2. as All cargo tanks were loaded with the same grade of cargo (homogeneous condition). The crude oil characteristic data are presented in table 6.2. The crude oil is heated at 30° Celsius in order to be discharged. The cross over valves of the cargo piping system are fully opened.

TABLE 6.1: Initial loading condition

Cargo Tank No.	Volume (m^3)
No.1 (P)	6370
No.1 (S)	6343
No.2 (P)	8095
No.2 (S)	8103
No.3 (P)	7724
No.3 (S)	7710
No.4 (P)	7585
No.4 (S)	6602
No.5 (P)	7873
No.5 (S)	7876
No.6 (P)	5577
No.6 (S)	5596
Slop (P)	956
Slop (S)	953

TABLE 6.2: Crude oil characteristic data.

Crude oil name:	Maya
API gravity:	21.1
RVP [psig]:	6.2
Kinematic viscosity at 30 ⁰ C [cst]:	30

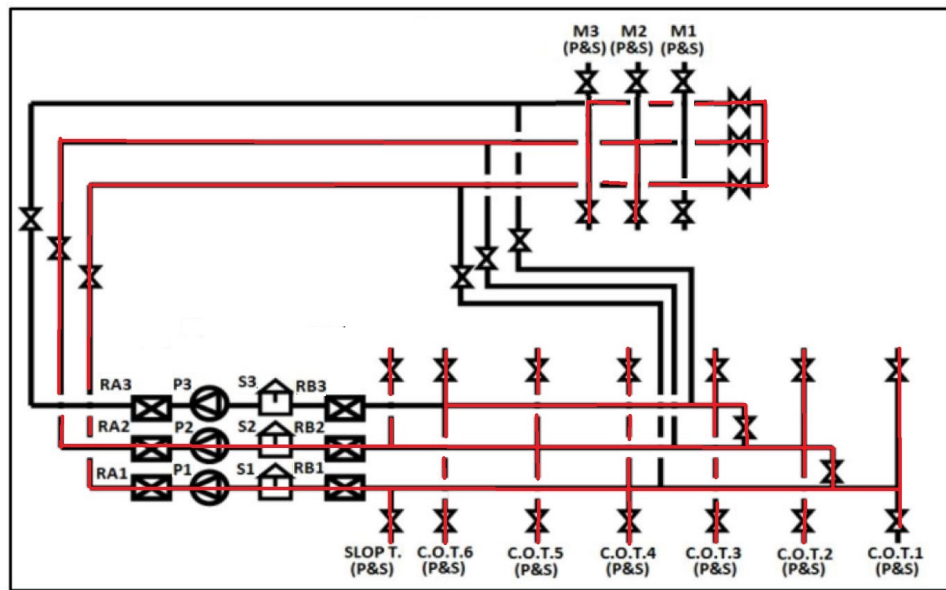


FIGURE 6.2: Involved piping network according to case study1 discharging plan.

6.2 Case study 2

The initial loading conditions of the cargo tanks are presented in table 6.3. The discharged crude oil is the same as in case study 1 (i.e. “Maya”, table 6.2). Two pumps were used working at 1220rpm. The cargo was discharged at the two of the three available manifolds. All cargo tanks were loaded with the same grade of cargo (homogeneous condition). The crude oil is heated at 30° Celsius in order to be discharged. The cross over valves of the cargo piping system are fully opened. It is worth noting that, the differences between case study 1 and 2 are the initial loading condition and the different rotational speed of the pumps. Moreover, the involved piping network (see figure 6.2) is the same as in case study 1.

TABLE 6.3: Initial loading condition

Cargo Tank No.	Volume (m^3)
No.1 (P)	6121
No.1 (S)	6116
No.2 (P)	7858
No.2 (S)	7855
No.3 (P)	7983
No.3 (S)	7997
No.4 (P)	8103
No.4 (S)	6856
No.5 (P)	8033
No.5 (S)	8041
No.6 (P)	5882
No.6 (S)	5888
Slop (P)	892
Slop (S)	897

6.3 Case study 3

The initial loading conditions of the cargo tanks are presented in table 6.5. The discharged crude oil is called “Olmeca” and its characteristic data are presented at table 6.4. Furthermore, there is no heat needed for this crude oil, in order to be discharged. Three cargo pumps were used working at 1050rpm. The cargo was discharged at the two of the three available manifolds. All cargo tanks were loaded with the same grade of cargo (homogeneous condition). This case study is completely different from the previous case studies. In this manner, the initial loading condition, the number of pumps in use, their rotational speed and the discharged cargo are different. The involved piping network according to case study 3 discharging plan, is illustrated in figure 6.3.

TABLE 6.4: Crude oil characteristic data.

Crude oil name:	Olmeca
API gravity:	39.15
RVP [psig]:	2.4
Kinematic viscosity at 20°C [cst]:	20

TABLE 6.5: Initial loading condition

Cargo Tank No.	Volume (m^3)
No.1 (P)	5107
No.1 (S)	5107
No.2 (P)	7809
No.2 (S)	7727
No.3 (P)	7578
No.3 (S)	7568
No.4 (P)	3861
No.4 (S)	3855
No.5 (P)	6550
No.5 (S)	6558
No.6 (P)	3504
No.6 (S)	3678
Slop (P)	565
Slop (S)	560

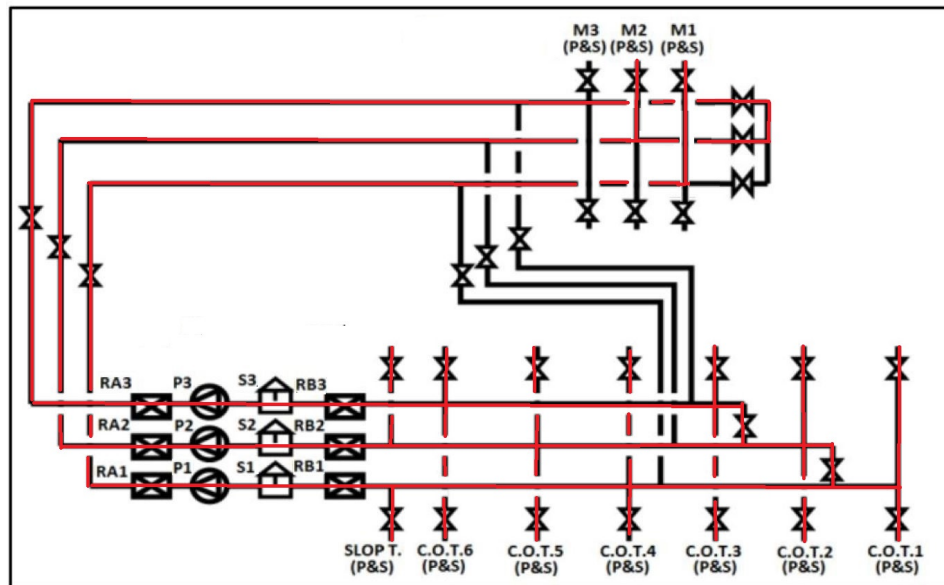


FIGURE 6.3: Involved piping network according to case study 2 discharging plan.

6.4 Results and discussion

The outputs of each case study are given in the form of the relevant pumping log and oil transfer plan, as presented in appendix B. The results for the hydraulic model, the ship's response and the fuel oil consumption are presented individually, since the further elaboration of the calculations is significant. Hence, the nominal characteristics, the behavior at partial load or actual service conditions can be evaluated and optimized.

Hydraulic system validation

The model has been validated by comparison of the calculated pressure at two critical points (i.e. after pumps and at manifolds) against actual pressure values for the same corresponding conditions and operation. It is necessary to ascertain that the pressures at these two points are the only officially recorded pressures during an actual discharging.

The resulted pressure values depend on how detailed is the overall design of the system regarding all included components, namely, the cargo tanks, the pumps, the shore tanks, the piping and fittings. The cargo tanks were modeled identically to the existing vessel's tanks, since all needed information was available, such as "Tank calibration tables" and general arrangement. The pumps were modeled by utilizing their characteristic curves and were checked against the operation of the existing pumps, in order to confirm them being identical. The characteristics of the shore piping network and the receiving tanks were accessed. Moreover, the piping network, including all its fitting, was modeled with respect to ship's general arrangement and its basic particulars. As a result, any deviation between the pressure values, at the manifolds and after the pumps, of the existing vessel and the model is due to the assumptions that were made at the development of the piping network (overestimation or underestimation of friction losses).

A good agreement between the calculated and actual pressure values, confirm the correct design and simulation of the system's hydraulic procedure. To this end, the pressures at the manifolds and the pressures after the pumps have been validated by comparing the calculated data against actual data, as presented in tables 6.4, 6.5, 6.6. Finally, it is necessary to ascertain that the model represents an ideal discharging procedure. Hence, any stoppages or throttling at valves, which are common practices in actual discharging procedures, were not considered. As a result, the discharged step at the actual procedures differs from the simulated discharging step.

CASE STUDY 1											
Actual measurements											
	pumps						manifolds			R.O.B	discharged step
	pump 1		pump 2		pump 3		manifold 1	manifold 2	manifold 3		
	rpm	pressure at disch.	rpm	pressure at disch.	rpm	pressure at disch.	pressure	pressure	pressure		
	1200	10.5	1200	10.5	-	-	-	8.5	8.5	385833.3	28340
	1200	10.5	1200	10.5	-	-	-	8.5	8.5	358232.3	27600.9
	1200	10.5	1200	10.5	-	-	-	8.5	8.5	331477.4	26755
AVERAGE	1200	10.5	1200	10.5				8.5	8.5	358514.3	27565.3
Calculated Results											
	pumps						manifolds			R.O.B	discharged step
	pump 1		pump 2		pump 3		manifold 1	manifold 2	manifold 3		
	rpm	pressure at disch.	rpm	pressure at disch.	rpm	pressure at disch.	pressure	pressure	pressure		
	1200	10.5	1200	10.5	-	-	-	8.5	8.5	378249.7	28244.6
	1200	10.5	1200	10.5	-	-	-	8.5	8.5	350204.7	28044.9
	1200	10.5	1200	10.4	-	-	-	8.5	8.5	322359.2	27845.6
AVERAGE	1200	10.5	1200	10.5				8.5	8.5	350271.2	28045.0
declination	0%	0%	0%	0%				0%	0%		2%

FIGURE 6.4: Calculated values regarding case study 1. The corresponding measurements are also included for comparison.

CASE STUDY 2											
Actual measurements											
	pumps						manifolds			R.O.B	discharged step
	pump 1		pump 2		pump 3		manifold 1	manifold 2	manifold 3		
	rpm	pressure at disch.	rpm	pressure at disch.	rpm	pressure at disch.	pressure	pressure	pressure		
	1220	10.8	1220	10.8	-	-	-	8.8	8.8	332481.9	28751.4
	1220	10.8	1220	10.8	-	-	-	8.8	8.8	304139.4	28342.5
	1220	10.8	1220	10.8	-	-	-	8.8	8.8	275308.1	28831.2
AVERAGE	1220	10.8	1220	10.8				8.8	8.8	303976.5	28641.7
Calculated Results											
	pumps						manifolds			R.O.B	discharged step
	pump 1		pump 2		pump 3		manifold 1	manifold 2	manifold 3		
	rpm	pressure at disch.	rpm	pressure at disch.	rpm	pressure at disch.	pressure	pressure	pressure		
	1220	10.9	1220	10.9	-	-	-	8.9	8.8	338493.4	30906.8
	1220	10.9	1220	10.8	-	-	-	8.9	8.8	307846.1	30647.2
	1220	10.8	1220	10.8	-	-	-	8.8	8.7	278187.1	29659.0
AVERAGE	1220	10.9	1220	10.8				8.9	8.8	308175.5	30404.3
declination	0%	1%	0%	0%				1%	0%		6%

FIGURE 6.5: Calculated values regarding case study 2. The corresponding measurements are also included for comparison.

CASE STUDY 3											
Actual measurements											
	pumps						manifolds			R.O.B	discharged step
	pump 1		pump 2		pump 3		manifold 1	manifold 2	manifold 3		
	rpm	pressure at disch.	rpm	pressure at disch.	rpm	pressure at disch.	pressure	pressure	pressure		
	1050	8	1050	8	1050	8	5	5	-	244400	40358
	1050	8	1050	8	1050	8	5	5	-	202366	42034
	1050	8	1050	8	1050	8	5	5	-	165194	37172
AVERAGE	1050	8	1050	8	1050	8	5	5		203986.7	39855
Calculated Results											
	pumps						manifolds			R.O.B	discharged step
	pump 1		pump 2		pump 3		manifold 1	manifold 2	manifold 3		
	rpm	pressure at disch.	rpm	pressure at disch.	rpm	pressure at disch.	pressure	pressure	pressure		
	1050	8.1	1050	8.1	1050	8.0	5.2	5.2	-	265948.8	41319.72
	1050	8.0	1050	8.0	1050	8.0	5.2	5.2	-	225217.6	40731.22
	1050	8.0	1050	8.0	1050	8.0	5.2	5.2	-	185074.9	40142.62
AVERAGE	1050	8.0	1050	8.0	1050.0	8.0	5.2	5.2		225414	40731
declination	0%	1%	0%	0%	0%	0%	4%	4%			2%

FIGURE 6.6: Calculated values regarding case study 3. The corresponding measurements are also included for comparison.

Stability and strength validation study

The validation study of vessel's stability and strength is achieved by comparison between the calculated results and the corresponding actual measurements. The loading conditions, as presented in the "Trim and stability booklet", are shown in tables 6.7, 6.6.

TABLE 6.6: Liquid transfer condition for MARPOL ANNEX I reg.27

Condition 2: Liquid transfer condition for MARPOL ANNEX I reg.27					
Deadweight items	weight	LCG from M/S	Moment about M/S	VCG above BL	Moment about BS
Bunker	4483.5	-83.31	-373520	15.29	68559
C.O.T. 1 (P)	6839.50	89.47	611930	12.03	82279
C.O.T. 1 (S)	6839.50	89.47	611930	12.03	82279
C.O.T. 2 (P)	8845.50	61.22	541535	11.83	104642
C.O.T. 2 (S)	8845.50	61.22	541535	11.83	104642
C.O.T. 3 (P)	8877.90	31.30	277878	11.83	105026
C.O.T. 3 (S)	8877.90	31.30	277878	11.83	105026
C.O.T. 4 (P)	8877.90	1.34	11896	11.83	105026
C.O.T. 4 (S)	8877.90	1.34	11896	11.83	105026
C.O.T. 5 (P)	8877.90	-28.62	-254085	11.83	105026
C.O.T. 5 (S)	8877.90	-28.62	-254085	11.83	105026
C.O.T. 6 (P)	6709.90	-55.31	-371125	12.21	81928
C.O.T. 6 (S)	6709.90	-55.31	-371125	12.21	81928
C.O.T. SLOP (P)	1074.40	-69.80	-74993	12.87	13828
C.O.T. SLOP (S)	1074.40	-69.80	-74993	12.87	13828
W.B.T 1 (P)	28.00	87.58	2452	0.05	1
W.B.T 1 (S)	28.00	87.58	2452	0.05	1
W.B.T 2 (P)	29.30	60.61	1776	0.03	1
W.B.T 2 (S)	29.30	60.61	1776	0.03	1
W.B.T 3 (P)	30.00	31.30	939	0.03	1
W.B.T 3 (S)	30.00	31.30	939	0.03	1
W.B.T 4 (P)	30.00	1.34	40	0.03	1
W.B.T 4 (S)	30.00	1.34	40	0.03	1
W.B.T 5 (P)	29.10	-27.91	-812	0.03	1
W.B.T 5 (S)	29.10	-27.91	-812	0.03	1
W.B.T 6 (P)	30.10	-55.80	-1680	0.05	2
W.B.T 6 (S)	30.10	-55.80	-1680	0.05	2
W.B.T FPT	17.20	109.82	1889	0.28	5
W.B.T APT	12.00	-107.89	-1295	9.71	117
Displacement	123933.00	7.58	939365	11.96	1482408

TABLE 6.7: Light Ship Condition

Condition 1: Light Ship Condition					
Deadweight items	weight	LCG from M/S	Moment about M/S	VCG above BL	Moment about BS
Bunker	0	0	0	0	0
Cargo	0	0	0	0	0
water ballast	0	0	0	0	0
deadweight	0	0	0	0	0
Lightweight	18861.8	-9.5	-179245	11.57	218231

Regarding the stability calculations, the calculated against the actual data are presented in table 6.8, with very good agreement.

TABLE 6.8: Calculated values regarding the Lightship and segregated ballast loading conditions. The corresponding measurements are also included for comparison.

Condition 1: Lightship			
	actual	calculated	declination
Displacement	18861.8	18862.0	0%
Trim	-4.17	-4.18	0%
Mean draught	2.8	2.79	0%
Condition 2: Liquid transfer condition for MARPOL ANNEX I reg.27			
	actual	calculated	declination
Displacement	123933.50	123933.50	0%
Trim	0.68	0.67	0%
Mean draught	15.03	15.3	0%

It is necessary to ascertain, that all stability calculations during the discharging procedure, are recorded hourly in the relevant “Oil transfer plan”. In this context, the stability calculations for each case study are presented in appendix B. It can be concluded that the discharging scenarios are with respect to the acceptable stability and strength limits.

As far as the strength calculations are concerned, the calculated against the actual data are presented in figures below:

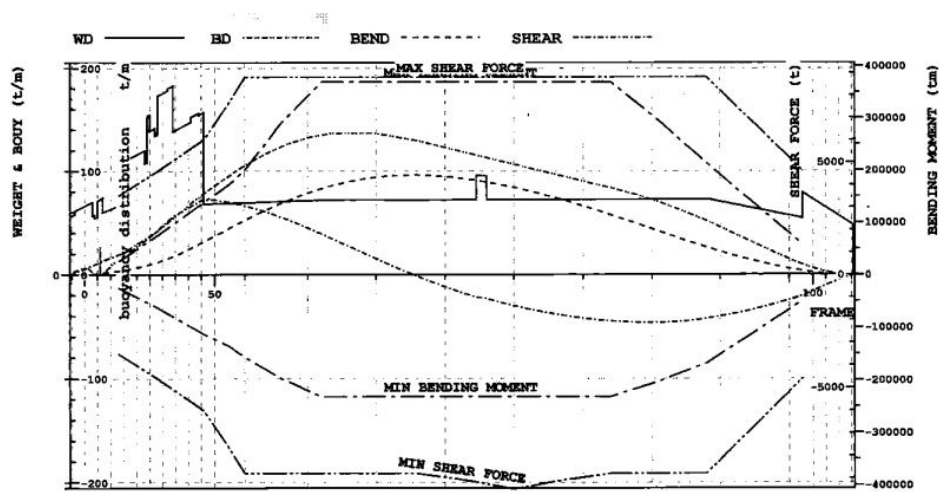


FIGURE 6.7: Strength distribution, as presented in the “Trim and stability booklet” for Lightship condition.

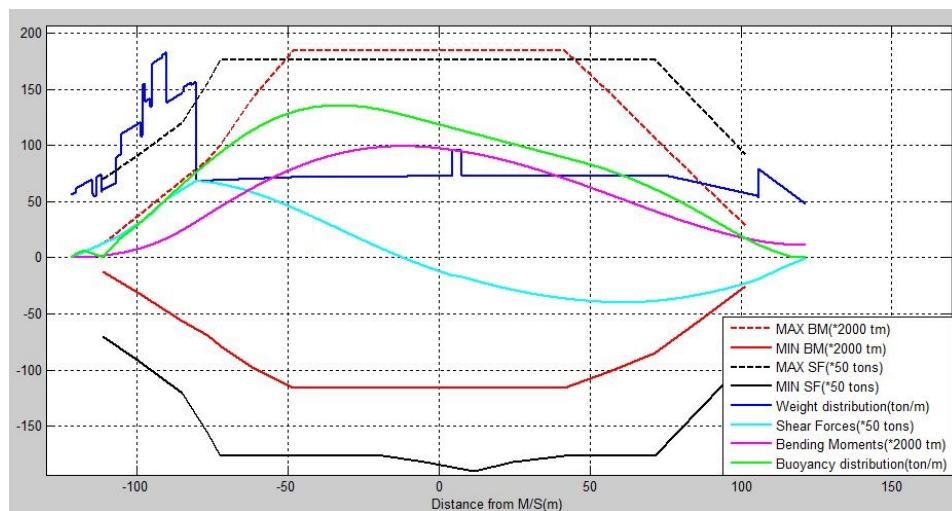


FIGURE 6.8: Strength distribution, as calculated in the present model for Lightship condition.

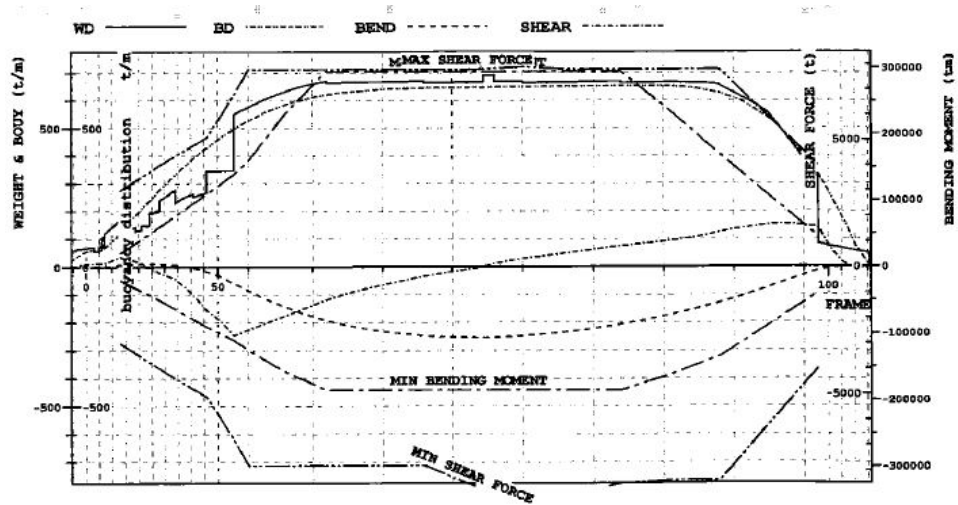


FIGURE 6.9: Strength distribution, as presented in the “Trim and stability booklet” for segregated ballast condition.

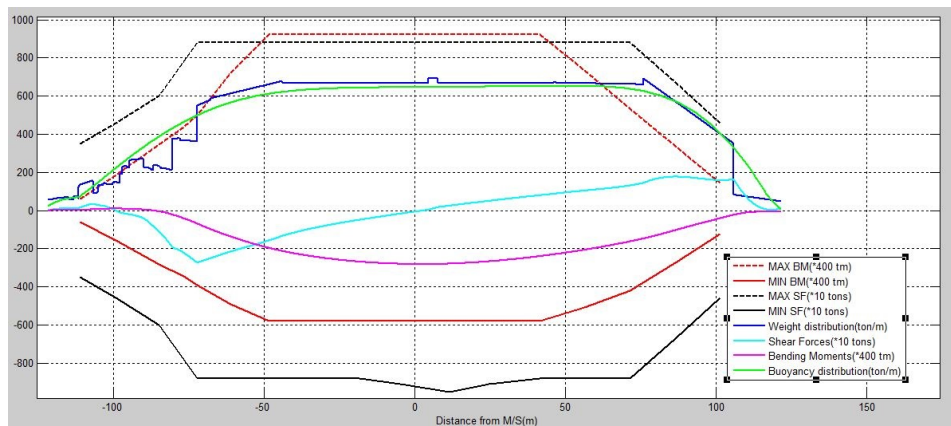


FIGURE 6.10: Strength distribution, as calculated in the model for segregated ballast condition.

Fuel consumption calculation

The calculation of the consumed fuel during the discharging procedure is considered important, and the present model utilizes the mathematical approach as described in section 5.3.3 to predict the boiler fuel consumption. Hence, the calculation of fuel consumption is based on the required steam capacity of cargo pumps, in order to utilize the relevant performance diagrams of boiler. The performance diagram regarding the steam capacity versus fuel consumption is shown in figure 6.11.

Actual measurements of boiler fuel consumption during vessel discharging procedure are not available, consequently, the validation of model predictions is not feasible at the present. The fuel oil consumption at the boilers, for each case study, is presented in appendix B.

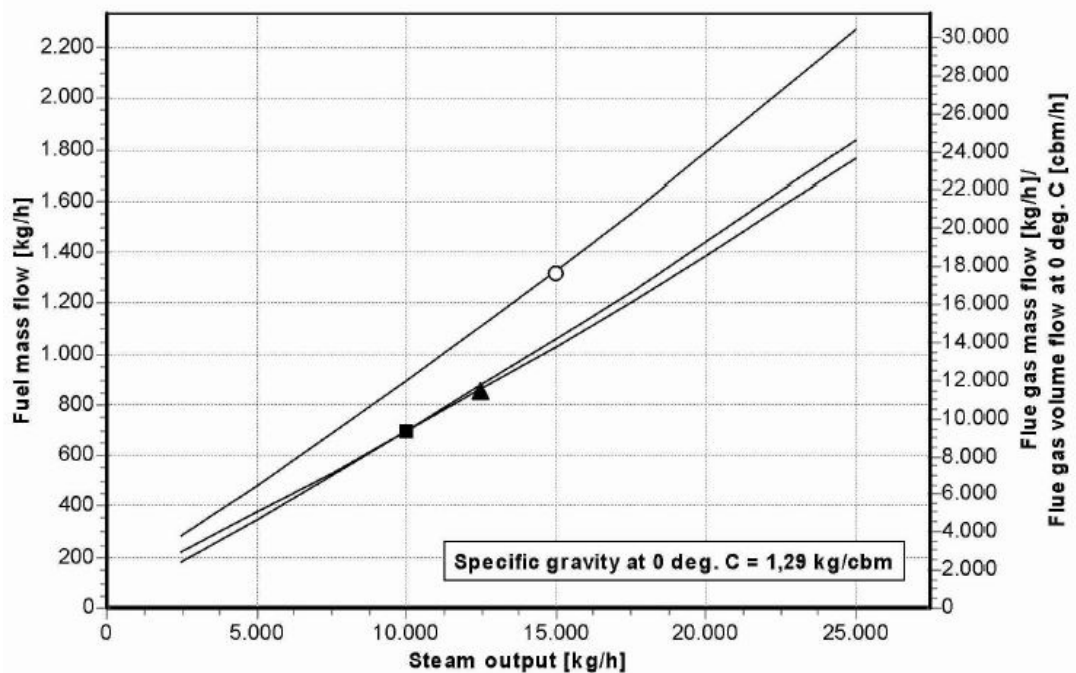


FIGURE 6.11: Boiler's fuel consumption as a function of the steam production given by manufacturer.

Chapter 7

Conclusions/Future work

Nowadays, the adverse international economic environment and the steep increase of fuel prices have severe impact on vessel's efficacy. Thus, the investigation of new technologies and operational procedures is required, so as vessel's energy efficiency to be improved. In this context, a detailed model that simulates the discharging procedure of crude oil tankers has been developed by the author. The model incorporates the structure constrains of the vessel, as well as the static and dynamic behavior of the crude oil, as it flows through the individual components of the hydraulic system (cargo and ballast piping diagrams). It is worth noting that the present model accounts for any tanker vessel, since the vessel's particulars are imposed in parametric form. The model calculates the required steam demand of cargo pumps and the corresponding fuel consumption of boilers, by taking into consideration the boiler performance curves. Different discharging scenarios are considered, in order the possibility of energy consumption optimization to be investigated. In addition, the present study includes parametric study of the following conditions: (a) initial vessel loading conditions (i.e. cargo and ballast tank volumes), (b) shore system characteristics (i.e. shore tank and shore piping particulars), (c) the discharging plan basic parameters (i.e. number of pumps in use, number of manifolds, rotational speed of the pumps, cargo properties).

Following the present study, future work can include the realistic spatial design of piping system, in order model accuracy to be further improved. The existing modeling of piping is based on the schematic general arrangement of the vessel. Thus, the provision of 3-D piping diagrams is required for the next steps, by suitable on board measurements. Further, actual measurements of the boiler fuel consumption are important for the validation of the calculated fuel consumption. Finally, the present model can be evolved as a decision support tool for the optimization of the discharging operation and the corresponding boiler fuel consumption.

Appendix A

Physical properties of fresh water

TABLE A.1: Physical properties of fresh water (SI units).

Temperature T(°C)	Specific Weight γ ($\frac{KN}{m^3}$)	Density ρ ($\frac{kg}{m^3}$)	Dynamic Viscos- ity μ ($10^{-3} \frac{kg}{msec}$)	Kinematic Viscos- ity ν ($10^{-6} \frac{m^2}{s}$)	Surface Tension σ ($\frac{N}{m}$)	Modulus of Elas- ticity E (* $10^9 \frac{N}{m^2}$)	Vapour Pressure P_v ($\frac{kN}{m^2}$)
0	9.805	999.8	1.781	1.785	0.0765	1.98	0.61
5	9.807	1000.0	1.518	1.519	0.0749	2.05	0.87
10	9.804	999.7	1.307	1.306	0.0742	2.10	1.23
15	9.798	999.1	1.139	1.139	0.0735	2.15	1.70
20	9.789	998.2	1.002	1.003	0.0728	2.17	2.34
25	9.777	997.0	0.890	0.893	0.0720	2.22	3.17
30	9.764	995.7	0.798	0.800	0.0712	2.25	4.24
40	9.730	992.2	0.653	0.658	0.0696	2.28	7.38
50	9.689	988.0	0.547	0.553	0.0679	2.29	12.33
60	9.642	983.2	0.466	0.474	0.0662	2.28	19.92
70	9.589	977.8	0.404	0.413	0.0644	2.25	31.16
80	9.530	971.8	0.354	0.364	0.0626	2.20	47.34
90	9.465	965.3	0.315	0.326	0.0608	2.14	70.10
100	9.399	958.4	0.282	0.294	0.0589	2.07	101.33

Source: Adapted from J.K Vernard and R.L Street (1975). *Elementary Fluid Mechanics*, 5th ed., Wiley, New York

TABLE A.2: Physical properties of fresh water (U.S. customary units)

Temperature T(°F)	Specific Weight γ ($\frac{lb}{ft^3}$)	Density ρ ($\frac{slug}{ft^3}$)	Dynamic Viscos- ity μ (*10 ⁻⁵ $\frac{lbs}{ft^2}$)	Kinematic Viscos- ity ν (*10 ⁻⁵ $\frac{ft^2}{s}$)	Surface Tension σ ($\frac{lb}{ft}$)	Modulus of Elas- ticity E (*10 ³ $\frac{lb}{in^2}$)	Vapour Pressure P_v ($\frac{lb}{in^2}$)
32	62.42	1.940	3.746	1.931	0.00518	287	0.09
49	62.43	1.940	3.229	1.664	0.00614	296	0.12
50	62.41	1.940	2.735	1.410	0.00509	305	0.18
60	62.37	1.938	2.359	1.217	0.00504	313	0.26
70	62.30	1.936	2.050	1.059	0.00498	319	0.36
80	62.22	1.934	1.799	0.930	0.00492	324	0.51
90	62.11	1.931	1.595	0.826	0.00486	328	0.70
100	62.00	1.927	1.424	0.739	0.00480	331	0.95
110	61.86	1.923	1.284	0.667	0.00473	332	1.27
120	61.71	1.918	1.168	0.609	0.00467	332	1.69
130	61.55	1.913	1.069	0.558	0.00460	331	2.22
140	61.38	1.908	0.981	0.514	0.00454	330	2.89
150	61.20	1.902	0.905	0.476	0.00447	328	3.72
160	61.00	1.896	0.838	0.442	0.00441	326	4.74
170	60.80	1.890	0.780	0.413	0.00434	322	5.99
180	60.58	1.883	0.726	0.385	0.00427	318	7.51
190	60.36	1.876	0.678	0.362	0.00420	313	9.34
200	60.12	1.868	0.637	0.341	0.00413	308	11.52
212	59.83	1.860	0.593	0.319	0.00404	300	14.70

The following equations (R.C. Weast, 1983, CRC Handbook of Chemistry and Physics, 64th edition, CRC Press, Boca Raton, FL) can be used to compute the density ρ_w ($\frac{kg}{m^3}$) and dynamic viscosity μ_w ($\frac{kg}{msec}$) at other temperatures.

$$\rho_w = \frac{999.83952 + 16.945176(T) - 7.987040110^{-3}(T)^2 - 46.17046110^{-6}(T)^3 + 105.5630210^{-9}(T)^4 - 280.5425310^{-12}(T)^5}{1 + 16.87985010^{-3}(T)} \quad (A.1)$$

For $0 < T < 20^\circ C$, $\mu_w = 10^{-3}(10^A)$

where $A = \frac{1301}{998.333 + 8.1855(T-20) + 0.00585(T-20)^2} - 1.30223$

For $0 < T < 100^\circ C$, $\mu_w = (1.00210^{-3}(10^B))$

where $B = \frac{1.3272(20-T) - 0.001053(T-20)^2}{T+105}$

Appendix B

Simulation results

TABLE B.1: Case study 1- Oil transfer plan (1)

Oil Transfer Plan					
TIME(hours)	1	2	3	4	5
Total Bbls	566341.0	581257.0	594935.9	606076.9	613999.6
Total M/T CARGO(m^3)	82908.2	78289.0	73702.2	69147.8	64625.5
Total M/T Ballast(Bbls)	44848.3	88819.3	131348.8	171137.2	207505.3
Draft F(m)	12.3	12.8	13.6	14.3	14.6
Draft A(m)	12.8	13.0	12.8	12.7	12.8
TRIM(m)	-0.5	-0.2	0.8	1.6	1.9
Max shear force(tons)	101154.6	104278.2	107195.3	109693.9	111663.3
Max bending moment($t*m$)	1155333177.2	1187890535.6	1209409878.3	1227663228.2	1247728112.8
Tank No(Bbls)					
CARGO 1P	36292.8	33821.7	31737.1	29747.1	27782.7
CARGO 1S	36083.0	33718.8	31663.0	29678.8	27716.0
CARGO 2P	47335.4	44569.4	41982.0	39461.8	36972.3
CARGO 2S	47248.9	44488.1	41910.1	39394.5	36907.0
CARGO 3P	47442.0	45276.0	42874.9	40414.5	37939.0
CARGO 3S	47471.8	45334.5	42946.9	40491.0	38016.9
CARGO 4P	44342.7	42180.8	39853.5	37445.2	35008.0
CARGO 4S	44026.1	42061.4	39724.3	37307.3	34866.6
CARGO 5P	45904.5	42731.5	39872.5	37199.9	34635.3
CARGO 5S	45802.1	42628.3	39783.0	37122.1	34564.8
CARGO 6P	35187.6	33583.1	31738.1	29797.9	27823.4
CARGO 6S	35192.4	33590.9	31747.9	29808.6	27834.4
CARGO SLOP P	4802.7	4374.4	3995.3	3639.9	3302.1
CARGO SLOP S	4360.6	4078.7	3758.5	3431.2	3125.7
BALLAST 1P	2103.7	4687.2	8061.9	11430.5	14556.4
BALLAST 1S	2103.7	4687.2	8061.9	11430.5	14556.4
BALLAST 2P	3240.0	7069.0	11001.5	13519.6	16363.3
BALLAST 2S	3240.0	7069.0	11001.5	13519.6	16363.3
BALLAST 3P	3464.3	7507.1	11477.0	13998.9	16848.1
BALLAST 3S	3464.3	7507.1	11477.0	13998.9	16848.1
BALLAST 4P	3913.1	8228.4	11656.4	14111.0	16925.7
BALLAST 4S	3913.1	8228.4	11656.4	14111.0	16925.7
BALLAST 5P	4529.9	8783.9	11337.6	13732.4	16510.0
BALLAST 5S	4622.9	9139.7	11873.4	14269.2	17046.7
BALLAST 6P	4857.3	7241.6	9726.4	13557.1	17000.5
BALLAST 6S	4857.3	7241.6	9726.4	13557.1	17000.5
BALLAST FPT	538.9	1429.0	4291.6	9901.5	10560.5
Fuel consumption(kg)	1758.7	3513.9	5266.0	7015.0	8760.8

TABLE B.2: Case study 1- Oil transfer plan (2)

Oil Transfer Plan					
TIME(hours)	6	7	8	9	10
Total Bbls	605399.3	577354.4	549508.8	521861.9	494412.6
Total M/T CARGO(m^3)	60135.1	55676.4	51249.5	46854.1	42490.1
Total M/T Ballast(Bbls)	227149.6	227149.6	227149.7	227149.7	227149.7
Draft F(m)	14.7	14.0	13.4	12.8	12.2
Draft A(m)	12.6	12.3	12.1	11.8	11.6
TRIM(m)	2.1	1.7	1.3	1.0	0.6
Max shear force(tons)	110935.4	107034.1	103160.5	99314.5	95496.1
Max bending moment($t*m$)	1235757611.6	1193820389.5	1152271882.5	1111080996.6	1070209522.9
Tank No(Bbls)					
CARGO 1P	25831.0	23891.6	21960.9	20040.3	18131.8
CARGO 1S	25765.2	23826.8	21896.7	19977.0	18069.3
CARGO 2P	34500.7	32046.2	29603.8	27174.3	24760.2
CARGO 2S	34436.5	31983.1	29541.4	27112.7	24699.5
CARGO 3P	35463.5	32997.1	30536.4	28088.2	25654.2
CARGO 3S	35541.4	33074.3	30613.2	28164.0	25729.2
CARGO 4P	32569.5	30140.3	27716.5	25306.4	22911.1
CARGO 4S	32428.1	30000.2	27577.2	25169.0	22775.6
CARGO 5P	32131.2	29671.6	27237.7	24821.9	22427.2
CARGO 5S	32064.8	29608.0	27175.5	24761.0	22367.5
CARGO 6P	25841.6	23864.4	21909.2	19972.7	18054.7
CARGO 6S	25852.7	23875.3	21919.8	19983.0	18064.4
CARGO SLOP P	2995.5	2693.9	2406.9	2140.9	1877.3
CARGO SLOP S	2827.9	2532.0	2263.9	2000.8	1741.0
BALLAST 1P	17171.9	17171.9	17171.9	17171.9	17171.9
BALLAST 1S	17171.9	17171.9	17171.9	17171.9	17171.9
BALLAST 2P	17962.0	17962.0	17962.0	17962.0	17962.0
BALLAST 2S	17962.0	17962.0	17962.0	17962.0	17962.0
BALLAST 3P	18410.5	18410.5	18410.5	18410.5	18410.5
BALLAST 3S	18410.5	18410.5	18410.5	18410.5	18410.5
BALLAST 4P	18410.5	18410.5	18410.5	18410.5	18410.5
BALLAST 4S	18410.5	18410.5	18410.5	18410.5	18410.5
BALLAST 5P	17873.7	17873.7	17873.7	17873.7	17873.7
BALLAST 5S	17873.7	17873.7	17873.7	17873.7	17873.7
BALLAST 6P	18466.1	18466.1	18466.1	18466.1	18466.1
BALLAST 6S	18466.1	18466.1	18466.1	18466.1	18466.1
BALLAST FPT	10560.5	10560.5	10560.5	10560.5	10560.5
Fuel consumption(kg)	10503.6	12243.2	13979.8	15713.3	17443.7

TABLE B.3: Case study 1- Oil transfer plan (3)

Oil Transfer Plan					
TIME(hours)	11	12	13	14	15
Total Bbls	467160.9	440106.1	413247.3	386584.7	360118.1
Total M/T CARGO(m^3)	38157.6	33856.3	29586.3	25347.4	21139.6
Total M/T Ballast(Bbls)	227149.7	227149.7	227149.7	227149.7	227149.7
Draft F(m)	11.6	11.0	10.4	9.8	9.2
Draft A(m)	11.3	11.1	10.8	10.6	10.3
TRIM(m)	0.3	-0.1	-0.4	-0.7	-1.0
Max shear force(tons)	91705.1	87941.5	84205.2	80496.2	76814.4
Max bending moment($t*m$)	1029762105.6	989669243.1	949880670.9	910539394.8	871557340.6
Tank No(Bbls)					
CARGO 1P	16229.4	14336.1	12470.3	10618.3	8774.5
CARGO 1S	16167.4	14275.3	12412.5	10561.3	8721.9
CARGO 2P	22353.9	19959.2	17572.5	15186.7	12804.2
CARGO 2S	22293.7	19899.7	17513.4	15127.7	12745.5
CARGO 3P	23222.4	20805.2	18395.8	15980.0	13575.9
CARGO 3S	23297.0	20878.7	18469.1	16053.4	13648.6
CARGO 4P	20522.5	18147.5	15781.4	13416.5	11068.1
CARGO 4S	20388.0	18014.8	15649.7	13285.1	10941.3
CARGO 5P	20042.7	17669.6	15309.9	12952.0	10612.1
CARGO 5S	19983.5	17611.2	15252.2	12894.5	10556.7
CARGO 6P	16181.5	14335.9	12519.9	10770.5	9050.6
CARGO 6S	16190.6	14344.7	12527.8	10777.8	9057.7
CARGO SLOP P	1629.7	1398.8	1168.9	956.3	755.5
CARGO SLOP S	1509.0	1279.8	1054.1	855.0	655.9
BALLAST 1P	17171.9	17171.9	17171.9	17171.9	17171.9
BALLAST 1S	17171.9	17171.9	17171.9	17171.9	17171.9
BALLAST 2P	17962.0	17962.0	17962.0	17962.0	17962.0
BALLAST 2S	17962.0	17962.0	17962.0	17962.0	17962.0
BALLAST 3P	18410.5	18410.5	18410.5	18410.5	18410.5
BALLAST 3S	18410.5	18410.5	18410.5	18410.5	18410.5
BALLAST 4P	18410.5	18410.5	18410.5	18410.5	18410.5
BALLAST 4S	18410.5	18410.5	18410.5	18410.5	18410.5
BALLAST 5P	17873.7	17873.7	17873.7	17873.7	17873.7
BALLAST 5S	17873.7	17873.7	17873.7	17873.7	17873.7
BALLAST 6P	18466.1	18466.1	18466.1	18466.1	18466.1
BALLAST 6S	18466.1	18466.1	18466.1	18466.1	18466.1
BALLAST FPT	10560.5	10560.5	10560.5	10560.5	10560.5
Fuel consumption(kg)	19171.1	20895.4	22616.8	24335.0	26050.3

TABLE B.4: Case Study 1- Pumping log

		Pumping log											
		Pumps						Manifolds					
		Pump 1		Pump 2		Pump 3		No.1	No.2	No.3			
TIME (sec)	rpm	$\frac{kg}{cm^2}$	rpm	$\frac{kg}{cm^2}$	rpm	$\frac{kg}{cm^2}$	rpm	$\frac{kg}{cm^2}$	$\frac{kg}{cm^2}$	$\frac{kg}{cm^2}$	R.O.B(bbls)	discharged step	discharged total
3600	1200	10.7	1200	10.6	0	0	0	0	8.7	8.6	521492.7648		
7200	1200	10.6	1200	10.6	0	0	0	0	8.6	8.6	492437.6934	29055.07	29055.07
10800	1200	10.6	1200	10.6	0	0	0	0	8.6	8.6	463587.0831	28850.61	57905.68
14400	1200	10.6	1200	10.6	0	0	0	0	8.6	8.5	434939.6741	28647.41	86553.09
18000	1200	10.5	1200	10.5	0	0	0	0	8.6	8.5	406494.233	28445.44	114998.53
21600	1200	10.5	1200	10.5	0	0	0	0	8.5	8.5	378249.682	28244.55	143243.08
25200	1200	10.5	1200	10.5	0	0	0	0	8.5	8.5	350204.7389	28044.94	171288.03
28800	1200	10.5	1200	10.4	0	0	0	0	8.5	8.5	322359.172	27845.57	199133.59
32400	1200	10.4	1200	10.4	0	0	0	0	8.5	8.4	294712.2225	27646.95	226780.54
36000	1200	10.4	1200	10.4	0	0	0	0	8.4	8.4	267262.9393	27449.28	254229.83
39600	1200	10.4	1200	10.3	0	0	0	0	8.4	8.4	240011.2746	27251.66	281481.49
43200	1200	10.3	1200	10.3	0	0	0	0	8.4	8.4	212956.4137	27054.86	308536.35
46800	1200	10.3	1200	10.3	0	0	0	0	8.4	8.3	186097.5847	26858.83	335395.18
50400	1200	10.3	1200	10.3	0	0	0	0	8.4	8.3	159434.9738	26662.61	362057.79
54000	1200	10.2	1200	10.2	0	0	0	0	8.3	8.3	132968.3893	26466.58	388524.38

TABLE B.5: Case study 2- Oil transfer plan (1)

Oil Transfer Plan					
TIME	1	2	3	4	5
Total Bbls	567171.7	580437.2	592022.9	601127.9	607071.5
Total M/T CARGO(m^3)	83040.3	78158.6	73239.1	68361.0	63524.0
Total M/T Ballast(Bbls)	44848.3	88819.3	131348.8	171137.2	207505.3
Draft F	12.1	12.6	13.3	13.8	14.1
Draft A	12.7	12.8	12.6	12.5	12.5
TRIM	-0.6	-0.3	0.6	1.4	1.6
Max shear force	100402.7	102780.9	104959.2	106726.5	107972.8
Max bending moment	1146709211.4	1171285569.7	1184848942.8	1195272089.5	1207610543.6
Tank No(Bbls)					
CARGO 1P	36404.1	33809.8	31572.2	29438.8	27339.5
CARGO 1S	36187.2	33677.8	31466.2	29339.0	27241.8
CARGO 2P	47422.9	44455.6	41636.0	38884.3	36165.4
CARGO 2S	47335.0	44363.1	41549.4	38800.9	36083.7
CARGO 3P	47541.9	45306.1	42748.6	40093.5	37404.7
CARGO 3S	47585.0	45380.9	42837.4	40188.1	37501.5
CARGO 4P	44250.8	41718.8	39099.7	36434.8	33767.1
CARGO 4S	43726.8	41519.8	38921.0	36254.6	33586.8
CARGO 5P	45762.4	42283.3	39124.8	36183.2	33367.3
CARGO 5S	45652.2	42165.0	39020.2	36089.7	33280.5
CARGO 6P	35394.6	33796.5	31860.0	29807.3	27710.6
CARGO 6S	35402.7	33808.4	31874.5	29822.8	27726.6
CARGO SLOP P	5065.6	4838.1	4626.0	4443.9	4303.9
CARGO SLOP S	4592.2	4494.9	4338.1	4209.5	4086.8
BALLAST 1P	2103.7	4687.2	8061.9	11430.5	14556.4
BALLAST 1S	2103.7	4687.2	8061.9	11430.5	14556.4
BALLAST 2P	3240.0	7069.0	11001.5	13519.6	16363.3
BALLAST 2S	3240.0	7069.0	11001.5	13519.6	16363.3
BALLAST 3P	3464.3	7507.1	11477.0	13998.9	16848.1
BALLAST 3S	3464.3	7507.1	11477.0	13998.9	16848.1
BALLAST 4P	3913.1	8228.4	11656.4	14111.0	16925.7
BALLAST 4S	3913.1	8228.4	11656.4	14111.0	16925.7
BALLAST 5P	4529.9	8783.9	11337.6	13732.4	16510.0
BALLAST 5S	4622.9	9139.7	11873.4	14269.2	17046.7
BALLAST 6P	4857.3	7241.6	9726.4	13557.1	17000.5
BALLAST 6S	4857.3	7241.6	9726.4	13557.1	17000.5
BALLAST FPT	538.9	1429.0	4291.6	9901.5	10560.5
Fuel consumption	1842.4	3680.7	5515.1	7345.5	9171.8

TABLE B.6: Case study 2- Oil transfer plan (2)

Oil Transfer Plan					
TIME	6	7	8	9	10
Total Bbls	596549.8	565643.0	534995.8	505336.8	475702.8
Total M/T CARGO(m^3)	58728.2	53814.5	48942.2	44226.9	39515.6
Total M/T Ballast(Bbls)	227149.6	227149.6	227149.7	227149.7	227149.7
Draft F	14.0	13.2	12.5	11.8	11.1
Draft A	12.3	12.0	11.7	11.4	11.1
TRIM	1.7	1.3	0.8	0.4	0.0
Max shear force	106530.8	101924.7	97356.1	92825.0	88331.9
Max bending moment	1187991156.1	1138600529.2	1089671931.3	1041261699.9	993382152.3
Tank No(Bbls)					
CARGO 1P	25259.1	23120.2	20996.1	18935.4	16868.4
CARGO 1S	25162.7	23024.8	20901.7	18841.9	16775.8
CARGO 2P	33470.9	30721.4	27990.8	25327.5	22659.3
CARGO 2S	33390.4	30641.7	27912.1	25249.4	22582.0
CARGO 3P	34711.2	31945.8	29192.8	26500.2	23797.6
CARGO 3S	34808.3	32043.0	29289.2	26596.2	23893.0
CARGO 4P	31106.8	28387.7	25687.3	23050.5	20414.7
CARGO 4S	30927.3	28209.7	25511.3	22875.9	20242.1
CARGO 5P	30636.3	27878.7	25160.5	22518.9	19879.2
CARGO 5S	30553.7	27798.4	25082.1	22441.6	19802.9
CARGO 6P	25601.6	23436.9	21292.2	19233.6	17210.7
CARGO 6S	25617.5	23452.4	21307.5	19247.9	17224.4
CARGO SLOP P	4172.4	4006.3	3847.8	3760.2	3675.9
CARGO SLOP S	3981.8	3826.3	3674.8	3608.0	3527.1
BALLAST 1P	17171.9	17171.9	17171.9	17171.9	17171.9
BALLAST 1S	17171.9	17171.9	17171.9	17171.9	17171.9
BALLAST 2P	17962.0	17962.0	17962.0	17962.0	17962.0
BALLAST 2S	17962.0	17962.0	17962.0	17962.0	17962.0
BALLAST 3P	18410.5	18410.5	18410.5	18410.5	18410.5
BALLAST 3S	18410.5	18410.5	18410.5	18410.5	18410.5
BALLAST 4P	18410.5	18410.5	18410.5	18410.5	18410.5
BALLAST 4S	18410.5	18410.5	18410.5	18410.5	18410.5
BALLAST 5P	17873.7	17873.7	17873.7	17873.7	17873.7
BALLAST 5S	17873.7	17873.7	17873.7	17873.7	17873.7
BALLAST 6P	18466.1	18466.1	18466.1	18466.1	18466.1
BALLAST 6S	18466.1	18466.1	18466.1	18466.1	18466.1
BALLAST FPT	10560.5	10560.5	10560.5	10560.5	10560.5
Fuel consumption	10994.1	12812.1	14626.1	16435.8	18241.3

TABLE B.7: Case study 2- Pumping log

Pumping log															
Pumps															
TIME (sec)	Pump 1		Pump 2		Pump 3		Manifolds			R.O.B (bbls)					
	rpm	$\frac{kg}{cm^2}$	rpm	$\frac{kg}{cm^2}$	rpm	$\frac{kg}{cm^2}$	No.1	No.2	No.3	discharged step	discharged total	discharged step	discharged total	discharged step	discharged total
3600	1220	11.1	1220	11.1	0	0	0	9.0	8.9	522323.5					
7200	1220	11.1	1220	11.0	0	0	0	9.0	8.9	491617.9	30705.6	30705.6	30705.6		
10800	1220	11.0	1220	11.0	0	0	0	9.0	8.9	460674.1	30943.8	30943.8	61649.4		
14400	1220	11.0	1220	11.0	0	0	0	9.0	8.9	429990.7	30683.4	30683.4	92332.8		
18000	1220	11.0	1220	10.9	0	0	0	8.9	8.8	399566.2	30424.5	30424.5	122757.3		
21600	1220	10.9	1220	10.9	0	0	0	8.9	8.8	369400.1	30166.1	30166.1	152923.4		
25200	1220	10.9	1220	10.9	0	0	0	8.9	8.8	338493.4	30906.8	30906.8	183830.1		
28800	1220	10.9	1220	10.8	0	0	0	8.9	8.8	307846.1	30647.2	30647.2	214477.3		
32400	1220	10.8	1220	10.8	0	0	0	8.8	8.7	278187.1	29659.0	29659.0	244136.3		
36000	1220	10.8	1220	10.8	0	0	0	8.8	8.7	248553.1	29634.0	29634.0	273770.3		
39600	1220	10.8	1220	10.7	0	0	0	8.8	8.7	219054.1	29499.0	29499.0	303269.3		
43200	1220	10.7	1220	10.7	0	0	0	8.8	8.7	189588.1	29466.0	29466.0	332735.3		
46800	1220	10.7	1220	10.7	0	0	0	8.7	8.6	160262.1	29326.0	29326.0	362061.3		
50400	1220	10.7	1220	10.6	0	0	0	8.7	8.6	130992.1	29270.0	29270.0	391331.3		

TABLE B.8: **Case study 3- Oil transfer plan (1)**

Oil Transfer Plan					
TIME	1	2	3	4	5
Total Bbls	107103.6	143376.3	178291.4	210556.8	239495.4
Total M/T CARGO(m^3)	62255.4	55510.9	48850.3	42281.2	35805.7
Total M/T Ballast(Bbls)	44848.3	88819.3	131348.8	171137.2	207505.3
Draft F	10.0	9.8	10.1	10.4	10.3
Draft A	11.0	11.3	11.0	10.7	10.7
TRIM	-1.1	-1.4	-0.9	-0.3	-0.4
Max shear force	83083.4	83512.7	83780.5	83681.7	83107.3
Max bending moment	945632617.5	955750910.7	951256635.0	942741076.3	936504824.5
Tank No(Bbls)					
CARGO 1P	27397.5	23843.0	20765.3	17598.2	14407.5
CARGO 1S	27144.3	23648.3	20593.5	17425.4	14234.1
CARGO 2P	40338.5	33680.3	28557.4	24071.1	19874.5
CARGO 2S	39815.7	33281.5	28287.6	23876.2	19711.6
CARGO 3P	39215.1	32914.5	27964.5	23503.1	19273.4
CARGO 3S	39492.2	33238.8	28235.9	23726.0	19470.5
CARGO 4P	27950.6	27727.2	25543.7	22330.4	18671.6
CARGO 4S	28071.5	27693.0	25404.9	22109.2	18399.0
CARGO 5P	36239.6	31411.6	26890.6	22485.8	18227.1
CARGO 5S	36111.8	31237.9	26712.7	22316.0	18066.4
CARGO 6P	22109.8	19748.4	16882.6	13813.6	10807.0
CARGO 6S	22115.4	19766.3	16906.2	13838.7	10829.6
CARGO SLOP P	3317.5	2736.2	2346.9	1937.3	1589.9
CARGO SLOP S	2266.7	2236.6	2084.5	1779.4	1470.8
BALLAST 1P	2103.7	4687.2	8061.9	11430.5	14556.4
BALLAST 1S	2103.7	4687.2	8061.9	11430.5	14556.4
BALLAST 2P	3240.0	7069.0	11001.5	13519.6	16363.3
BALLAST 2S	3240.0	7069.0	11001.5	13519.6	16363.3
BALLAST 3P	3464.3	7507.1	11477.0	13998.9	16848.1
BALLAST 3S	3464.3	7507.1	11477.0	13998.9	16848.1
BALLAST 4P	3913.1	8228.4	11656.4	14111.0	16925.7
BALLAST 4S	3913.1	8228.4	11656.4	14111.0	16925.7
BALLAST 5P	4529.9	8783.9	11337.6	13732.4	16510.0
BALLAST 5S	4622.9	9139.7	11873.4	14269.2	17046.7
BALLAST 6P	4857.3	7241.6	9726.4	13557.1	17000.5
BALLAST 6S	4857.3	7241.6	9726.4	13557.1	17000.5
BALLAST FPT	538.9	1429.0	4291.6	9901.5	10560.5
Fuel consumption	2520.4	5031.4	7531.7	10020.3	12496.9

TABLE B.9: **Case study 3- Oil transfer plan (2)**

Oil Transfer Plan				
TIME	6	7	8	9
Total Bbls	251803.8	244560.9	237412.2	230368.3
Total M/T CARGO(m^3)	29423.7	23134.6	16939.8	10849.8
Total M/T Ballast(Bbls)	227149.6	227149.6	227149.7	227149.7
Draft F	9.9	8.9	8.0	7.0
Draft A	10.3	9.8	9.4	9.0
TRIM	-0.4	-0.9	-1.4	-2.0
Max shear force	79889.6	73552.0	67296.9	61133.5
Max bending moment	898846693.9	832015411.9	766084772.6	702348202.0
Tank No(Bbls)				
CARGO 1P	11248.2	8135.7	5178.9	2259.1
CARGO 1S	11080.2	7985.5	5043.4	2135.9
CARGO 2P	15780.6	11708.6	7633.5	3473.6
CARGO 2S	15629.5	11562.2	7489.0	3331.7
CARGO 3P	15143.1	11042.8	6948.9	2720.1
CARGO 3S	15328.4	11221.7	7125.5	2898.0
CARGO 4P	14810.3	10861.1	6855.4	2785.2
CARGO 4S	14509.4	10550.2	6538.0	2475.5
CARGO 5P	14076.5	9993.6	5942.5	1877.1
CARGO 5S	13922.8	9846.8	5801.8	1740.0
CARGO 6P	7920.6	5209.8	2627.4	1090.2
CARGO 6S	7940.5	5227.0	2641.5	1090.2
CARGO SLOP P	1271.5	987.0	732.9	0.0
CARGO SLOP S	1182.9	907.8	669.9	0.0
BALLAST 1P	17171.9	17171.9	17171.9	17171.9
BALLAST 1S	17171.9	17171.9	17171.9	17171.9
BALLAST 2P	17962.0	17962.0	17962.0	17962.0
BALLAST 2S	17962.0	17962.0	17962.0	17962.0
BALLAST 3P	18410.5	18410.5	18410.5	18410.5
BALLAST 3S	18410.5	18410.5	18410.5	18410.5
BALLAST 4P	18410.5	18410.5	18410.5	18410.5
BALLAST 4S	18410.5	18410.5	18410.5	18410.5
BALLAST 5P	17873.7	17873.7	17873.7	17873.7
BALLAST 5S	17873.7	17873.7	17873.7	17873.7
BALLAST 6P	18466.1	18466.1	18466.1	18466.1
BALLAST 6S	18466.1	18466.1	18466.1	18466.1
BALLAST FPT	10560.5	10560.5	10560.5	10560.5
Fuel consumption	14961.6	17414.5	19855.3	22282.8

TABLE B.10: Case study 3- Pumping log

Pumping log													
Pumps													
TIME (sec)	Pump 1		Pump 2		Pump 3		Manifolds			R.O.B (bbls)			discharged total
	rpm	$\frac{kg}{cm^2}$	rpm	$\frac{kg}{cm^2}$	rpm	$\frac{kg}{cm^2}$	No.1	No.2	No.3	No.1	No.2	No.3	
3600	1050	8.1	1050	8.1	1050	8.1	5.2	5.2	0	391586.3039			
7200	1050	8.1	1050	8.1	1050	8.1	5.2	5.2	0	349163.4975			42422.81
10800	1050	8.1	1050	8.1	1050	8.1	5.2	5.2	0	307268.5044			41894.99
14400	1050	8.1	1050	8.1	1050	8.0	5.2	5.2	0	265948.782			41319.72
18000	1050	8.0	1050	8.0	1050	8.0	5.2	5.2	0	225217.5663			40731.22
21600	1050	8.0	1050	8.0	1050	8.0	5.2	5.2	0	185074.9441			40142.62
25200	1050	8.0	1050	8.0	1050	8.0	5.2	5.2	0	145516.4779			39558.47
28800	1050	8.0	1050	7.9	1050	7.9	5.2	5.2	0	106551.2569			38965.22
32400	1050	7.9	1050	7.9	1050	7.9	5.1	5.1	0	68245.28403			38305.97

Bibliography

- [1] IMO. “*Marpol Annex VI for Emission Control Areas*”. International Maritime Organisation, May 2005, .
- [2] IMO. “*International Convention for Ballast Water Management applicable from 2016*”. International Maritime Organisation, February 2004, .
- [3] Hamburg Ship Model Basin and Det Norske Veritas. “*Fuel Saving Guideline for Tankers*”. HSVA and DNV, Rev.1a, 2013.
- [4] REFRESH EU funded project. FP7-SST-2011-RTD-1 (285708). <http://www.refreshproject.eu>, 2012-2015.
- [5] Oil companies international marine forum and International chamber of shipping. “*ISGOTT International Safety Guide for Oil Tankers and Terminals*”. Witherby and Co LTD, fifth edition, 2006.
- [6] Custodio A. Bachus L. “*Know and Understand Centrifugal Pumps*”. Elsevier Ltd., 2003.
- [7] Gunner T.J. “*An explanation and guideline for pumping calculations*”. INTER-TANKO, March 2001.
- [8] The engineeringtoolbox website: Resources, tools and basic information for engineering and design of technical applications. http://www.engineeringtoolbox.com/pressure-d_587.html, .
- [9] Adamopoulos N. “*Pumping Calculations and Under-Performance Evaluation in Crude Oil Tankers*”. SNAME greek section, 4th International Symposium on Ship Operations,2012.
- [10] Grundfos. “*The Centrifugal Pump*”. Grundfos Research and Technology, 2013.
- [11] Hyperphysics website:. <http://hyperphysics.phy-astr.gsu.edu/hbase/pber.html>, .

- [12] Tzabiras G. “*Numerical simulations of hydrodynamic flows (in greek)*”. National Technical University of Athens, 2009.
- [13] Crane. “*Flow of fluids through valves, fittings and pipes*”. Crane Co., 1972.
- [14] American Bureau of Shipping(ABS). “*Rules for Building and Classing Steel Vessels*”. August 1997.
- [15] Energy institute hmc-4 oil transportation measurement committees website for crude oil measurement and property data.: <http://www.oil-transport.info>, .
- [16] International Maritime Organization website.: <http://www.imo.org>.
- [17] IMO. “*International Convention for the Prevention of Pollution from Ships (MARPOL)*”. International Maritime Organisation, sixth edition,2006, .
- [18] IMO. “*International Convention on Load Lines (LL)*”. International Maritime Organisation, 1966, .
- [19] IMO. “*International Convention for the safety of Life at Sea (SOLAS)*”. International Maritime Organisation,1960 and 1974, .
- [20] Derrett D.R. Barrass B. “*Ship Stability for Masters and Mates*”. Elsevier LTD.,sixth edition, 2006.
- [21] Samouilidis E. “*Ship’s Resistance*”(in Greek). National Technical University of Athens, 2011.
- [22] Nautical site website.: <http://thenauticalsite.com>.
- [23] Papanikolaou A. Adamopoulos N. Pytharoulis M. Plessas T., Boulougouris E. “*Simulation of Loading/Discharging Procedure of Tankers*”. 15th International Congress of the International Maritime Association of the Mediterranean, 2013.
- [24] U.S. Department) from wikipedia website: API gravity information(sources: Crude-monitor.ca, Canadian Centre for Energy Information. http://en.wikipedia.org/wiki/API_gravity.